

MARKO PART

Combined three-dimensional
sol-gel structures and atomic layer
deposited thin films



MARKO PART

Combined three-dimensional
sol-gel structures and atomic layer
deposited thin films



This study was carried out at the Institute of Physics, University of Tartu.

The dissertation was admitted on 23.02.2017 in partial fulfilment of the requirements for the degree of Doctor of Philosophy in materials science, and was allowed for defence by the Scientific Council on Materials Science of the University of Tartu.

Supervisors: Dr. Kaupo Kukli
Institute of Physics, University of Tartu, Estonia

Dr. Tanel Tätte
Institute of Physics, University of Tartu, Estonia

Opponents: Prof. Habil. Dr. Aivaras Kareiva
Vilnius University

Dr. Valdek Mikli
Tallinn University of Technology

Defence: March 30th, 2017 at University of Tartu, Estonia

This work was supported by the following agencies and foundations: Graduate School „Functional materials and technologies“ (European Social Fund project 1.2.0401.090079); ETF9292 „Combined sol-gel and solid-liquid phase separation processes in elaboration of novel shaped metal oxide nanoceramics.“; ETF8377 „Elaboration of tubular microstructures by controlled plastic-elastic transformation of alkoxide surfaces“; SF0180058s07 „Low-dimensional structures and their applications“; SF0180042s07 „Layered structures of solid films for information technology and nanoelectronics“; ETF7612 „Micro and nanosize metal oxide fibres“; TK141 „Advanced materials and high-technology devices for sustainable energetics, sensorics and nanoelectronics“; IUT2-24 „Thin-film structures for nanoelectronic applications and functional coatings“



European Union
European Regional
Development Fund



Investing
in your future

ISSN 2228-0928

ISBN 978-9949-77-360-2 (print)

ISBN 978-9949-77-361-9 (pdf)

Copyright: Marko Part, 2017

University of Tartu Press
www.tyk.ee

TABLE OF CONTENTS

| | |
|---|-----|
| LIST OF ORIGINAL PUBLICATIONS | 6 |
| AUTHOR'S CONTRIBUTION | 7 |
| LIST OF ABBREVIATIONS AND SYMBOLS | 8 |
| 1. INTRODUCTION | 9 |
| 2. AIM OF THE WORK | 11 |
| 3. BACKGROUND AND OBJECTIVES | 12 |
| 3.1. History of sol-gel chemistry | 12 |
| 3.2. Principles of sol-gel chemistry | 15 |
| 3.3. Chemistry of sol-gel processing | 15 |
| 3.4. Transition metal oxides | 20 |
| 3.5. Formation of metal-oxo-nanoparticles | 24 |
| 3.2.1. Preparation of molecular precursor | 26 |
| 3.2.2. Aging | 28 |
| 3.2.3. Drying | 28 |
| 3.2.4. Thermal treatment | 30 |
| 3.6. Microtubes | 33 |
| 4. THIN FILM DEPOSITION TECHNIQUES | 36 |
| 4.1. Atomic layer deposition | 37 |
| 5. RESULTS AND DISCUSSION | 40 |
| 5.1. Precursor materials | 40 |
| 5.1.1. Preparation of metal-oxo-alkoxide sols | 40 |
| 5.1.2. Formation, structure and chemistry of metal alkoxides based sol-precursors | 40 |
| 5.1.3. Fibres vs. Tubes drawing | 42 |
| 5.2. Post-processing: monitoring of structure and properties during the aging and heat treatment of fibres and tubes | 44 |
| 5.2.1. Functional properties and applications of final materials | 45 |
| 6. SUMMARY AND CONCLUSIONS | 47 |
| 7. SUMMARY IN ESTONIAN | 48 |
| 8. ACKNOWLEDGEMENTS | 50 |
| 9. REFERENCES | 51 |
| 10. PUBLICATIONS | 65 |
| CURRICULUM VITAE | 160 |
| ELULOOKIRJELDUS | 161 |

LIST OF ORIGINAL PUBLICATIONS

- I. T. Tätte, M. Hussainov, M. Paalo, **M. Part**, R. Talviste, V. Kiisk, H. Mändar, K. Põhako, T. Pehk, K. Reivelt, M. Natali, J. Gurauskis, A. Lõhmus, U. Mäeorg, Alkoxide-based precursors for direct drawing of metal oxide micro- and nanofibres, *Sci. Technol. Adv. Mater.*, 12 (2011) 034412.
- II. T. Tätte, A. L. Kolesnikova, M. Hussainov, R. Talviste, R. Lõhmus, A. E. Romanov, I. Hussainova, **M. Part**, A. Lõhmus, Crack formation during post-treatment of nano- and microfibrils by sol-gel technique, *J. Nanosci. Nanotechnol.*, 10 (2010) 6009–6016.
- III. K. Hanschmidt, T. Tätte, I. Hussainova, **M. Part**, H. Mändar, K. Roosalu, I. Chasiotis, Optimization of mechanical strength of titania fibers fabricated by direct drawing, *Appl. Phys. A*, 113 (2013) 663–671.
- IV. **M. Part**, K. Hanschmidt, J. Jõgi, E. Rauwel, G. A. Seisenbaeva, V. G. Kessler, T. Tätte, Study of the curing mechanism of metal alkoxide liquid threads for the synthesis of metal oxide fibers or microtubes, *RSC Adv.*, 4 (2014) 12545–12554.
- V. T. Tätte, **M. Part**, R. Talviste, K. Hanschmidt, K. Utt, U. Mäeorg, I. Jõgi, V. Kiisk, H. Mändar, G. Nurk, P. Rauwel, Yttria stabilized zirconia microtubes for microfluidics under extreme conditions, *RSC Adv.*, 4 (2014) 17413–17419.
- VI. K. Utt, **M. Part**, T. Tätte, V. Kiisk, M. G. Brik, A. A. Chaykin, I. Sildos, Spectroscopic properties of Eu-doped Y-stabilized ZrO₂ microtubes, *J. Lumin.*, 152 (2014) 125–128.
- VII. **M. Part**, A. Tamm, J. Kozlova, H. Mändar, T. Tätte, K. Kukli, Atomic layer deposition of MgO films on yttria-stabilized zirconia microtubes, *Thin Solid Films*, 553 (2014) 30–32.
- VIII. Invention: A Method of Preparing Metal Oxide Microtubes; Tanel Tätte, **Marko Part**, Uno Mäeorg, Valter Kiisk, Gunnar Nurk, Aleksei Vorobjov, Kelli Hanschmidt Priority number: P201000097; Priority date: 31.12.2010.

AUTHOR'S CONTRIBUTION

- I. The author was responsible for preparing the sol-gel samples and for thermal treatment of the samples.
- II. The author was responsible for preparation of the sol-gel samples, for the thermal treatment of the samples and taking pictures with optical microscope.
- III. The author was responsible for preparing the sol-gel samples, for thermal treatment of the samples, and for the XRD and SAXS measurements.
- IV. The author planned and made the experiments for the preparation of sol-gel samples. The author did the optical and scanning electron microscopy measurements.
- V. The author was responsible for preparing the samples and for thermal treatment of the samples. The author also did optical microscopy measurements and XRD measurements.
- VI. The author was responsible for preparing the sol-gel samples and for thermal treatment of the samples.
- VII. The author made sol-gel structures. The author planned and made the film growth experiments. The author did the XRD and XRR measurements and electron microscopy measurements.
- VIII. The author was responsible for preparing the sol-gel samples and for thermal treatment of the samples. The author also did the XRD measurements and mechanical testing.

Author contributed to the preparation of all original papers.

LIST OF ABBREVIATIONS AND SYMBOLS

| | |
|---------|--|
| AFM | atomic force microscope |
| ALD | atomic layer deposition |
| ALE | atomic layer epitaxy |
| CVD | chemical vapor deposition |
| CMOS | complementary metal oxide semiconductor |
| CSD | chemical solution deposition |
| ECD | electroplating |
| EDX | energy dispersive X-ray spectrometry |
| FTIR | Fourier transform infrared spectroscopy |
| GIXRD | grazing incidence X-ray diffraction |
| GPC | grwth per cycle |
| HRTEM | high-resolution transmission electron microscope |
| MBE | molecular beam epitaxy |
| MEMS | micro-electro-mechanical system |
| MTSAL | micelles templated by self-assembly of ligands |
| NEMS | nano-electro-mechanical system |
| NMR | nuclear magnetic resonance |
| PLD | pulsed laser deposition |
| PVD | physical vapor deposition |
| SAXS | small angle X-ray scattering |
| SEM | scanning electron microscope |
| SEM-FIB | scanning eelctron microscope with ion beam |
| SOFC | solid oxide fuel cell |
| TEM | transmission electron microscope |
| TEOS | tetraethyl orthosilicate |
| TMOS | tetramethyl orthosilicate |
| UV | ultraviolet |
| VPE | vapor phase epitaxy |
| XPS | X-ray photoelectron spectroscopy |
| XRD | X-ray diffraction |
| XRR | X-ray reflectometry |
| YSZ | yttria-stabilized zirconia |

1. INTRODUCTION

Miniaturization of technological solutions, important in our everyday life, especially micro electro-mechanical systems (MEMS), has attracted tremendous attention as smaller systems possess higher efficiencies, quicker responses, lower cost, etc. The type of MEMSs would include systems from simple electro-mechanical switches to highly complexed ones. When the device will be used for transporting liquids and/or gases then tubular geometry is very often preferable in construction as it enables better thermomechanical behaviour and sealing simplicity compared to the use of channels etched into substrate. Tubular geometry enables also more uniform flowing of matter, compared to different shape of cross-sectional area. Microtubular fluidic systems are the tools rapidly developed to uncover new scientific solutions and challenges in a broad range of areas, such as: medical technology, biotechnology, chemical industry, environmental protection, electronic industry, fuel production and processing etc.

Under extreme conditions like elevated temperature (up to 1000 °C), pressure (hundreds of atmospheres) or plasma, the use of ceramics made microtubes or capillaries has no alternatives. An excellent composition material for such applications is yttria-stabilized zirconia (YSZ) that, in addition to the outstanding thermo-mechanical behaviour, finds its functionality due to its ionic conductance as ionic membrane in high temperature (operated at 700–1000 °C) solid oxide fuel cells. In addition, high surface to volume ratio of microscale tubes, heat transfer is highly efficient in devices constructed of these materials. Therefore, the temperature of microtubes based microreactors can simply be regulated by heat exchange.

A variety of different methods have been developed to fabricate microtubes made of various kinds of materials. The logic of template-based approaches is coating of cylindrical shape fine fibers, nano- and microrods, carbon filaments and nanotubes, etc. with desired material. Hollow microtubes will be prepared after removal of template from the core of structures. Usually it is achieved by oxidizing at elevated temperature or dissolving the core out in proper solvents. The main drawback of the approach is related to difficulties in removal of the template that would easily lead to cracking of the tube. The method, rather universal, however, is quite ineffective in terms of cost as the preparation of tubes in this manner consists of many steps: fabrication of template, coating of template, removal of template. Another, also a widely used technique is direct extrusion, which represents a straightforward and facile route to the production of long slender fiber structures, including also the hollow ones. Due to its simplicity, it has been widely used to produce microtubes in a cost-effective way. However, this technology cannot be applied to produce ceramic microtubes with diameter below 0,5 mm due to the collapse of the structures under critically high forces of surface tension.

In many cases, the tubes prepared by the methods described above require functional coatings (electrodes, different isolators, reflectors, catalysing films, etc.) on the inner and/or the outer surfaces. This coating would add new functionality for the tubes as well as improve their thermo-mechanical properties by filling the pores and critical cracks on the surface. Unfortunately, the task cannot be achieved by using simple wet chemical methods because of complications with the drying process. However, due to the high thermo-mechanical and chemical stability of ceramic materials, the tubes can be coated by atomic layer deposition (ALD) with the desired materials. That method is probably the best one to deposit subnanometer thick metal oxide or metal films uniformly on the surface of microtubes to give them additional functionality, for example by placing electrodes on the surface or just to make them mechanically more stable by filling unwanted pores and cracks in the tube material. ALD is a technique that, in its most general form, can be defined as a sequential, self-limiting, deposition process that operates on the principle of alternating saturating surface reactions.

The main purpose of the current thesis is to let the readers know about a novel self-assembly based synthesis method for the preparation of nanohomogeneous yttria-stabilized zirconia microtubes. The method is described in 2 research papers, published in RSC Advances and patented by the University of Tartu. To the best of our knowledge, there are no alternative methods for the synthesis of nanohomogeneous ceramic metal oxide microtubes in that low dimensions. The formation mechanism of the tubes is thoroughly discussed and the properties of final materials are studied in detail. We will pay attention on mechanical properties of the final materials: tensile strength and Young's modulus of the tubes have been measured. Optical characterisation of the tubes demonstrated their nanohomogeneity – the tubes were transparent structures with optical waveguiding properties and luminescent. Ionic conductance without electronic component was demonstrated at elevated temperatures, etc. An additional functionality of the tubes was achieved by ALD of MgO on the surface of achieved structures. The tubes will be demonstrated in some final applications as miniature solid oxide fuel cells and single tube based plasma devices.

2. AIM OF THE WORK

The main goal of the present study was to develop a technique for preparation of metal oxide microtubes applicable in high temperature and high pressure applications. There exists many different techniques for preparation of microscopic tubular structures, for example: template method, laser deposition, electrophoretic deposition etc.

Present method differs from beforementioned methods in many aspects. Firstly, this is fully sol-gel based method, which allows to use relatively low sintering temperatures and to produce materials with different shape and morphology. Secondly, due to high purity of precursor materials, obtained three-dimensional materials also exhibit very high purity degree. Thirdly, compared with other methods, sol-gel technique is relatively cost effective.

The second goal was to functionalize obtained microtubes with thin metal oxide films using atomic layer deposition. More precisely, the aim of this task was to investigate, whether the atomic layer deposition is suitable technique to grow thin films onto the inner and outer surface of metal oxide microtubes.

3. BACKGROUND AND OBJECTIVES

3.1. History of sol-gel chemistry

Ceramic materials are defined as inorganic non-metallic materials, consisting of compounds of a metal and a nonmetal elements (metal oxides, nitrides, carbides – both crystalline and amorphous) [1]. Due to their highly functional properties such as hardness, high porosity, and dielectric constant, ceramics are widely used in a broad range of applications, such as micro- and ultrafiltration, gas separation, protective and optical coatings, insulators, dielectric and electronic coatings, optical fibers [2, 3].

In recent decades, the number of works about synthesis of micro- and nanostructured ceramic materials, has met enormous growth [4–9]. In addition to nitrides, carbides, and borates, metal oxides are probably the most interesting group of materials in the form of nano and microstructured ceramics due to their several extreme properties, availability etc. So far, the most widely used technique in the synthesis of ceramic metal oxide materials in bulk has been based on hot powder pressing, followed by high-temperature sintering. In this method, the diffusion of the atomic and ionic species of the reactants is essential for the reaction to proceed. In order to provide high mobility of reaction partners, solid state processes usually require microscale particle sizes in neat powders and high temperatures up to thousands of Celsius degrees. These rough process conditions lead directly to thermodynamically stable phases without any intermediary metastable phases. However, in comparison with an alternative approach, i.e. the so-called *wet* or sol-gel chemistry, the sintering method can be considered as a rather crude approach for preparation of materials [10]. Wet chemical methods are used for the synthesis of nano and micro homogeneous ceramics and they are based on a controllable chemical build-up of structures from molecular precursors by breaking and forming bonds between the particles.

In the case of metal oxide ceramics, a special attention is paid to their preparation in the form of fine as well as hollow fibres, also called as micro capillaries or tubes. When the dimensions of the materials in process reach microscale then the conventional powder pressing and sintering are of no use. This is due to the rather big microscale particle sizes of used neat powder. A solution for the drawback is *wet* chemistry that offers the possibility to obtain shaped materials directly from molecular level from homogeneous solutions at relatively low (room) temperatures [11–14] and allows one to prepare materials with desired size and shape also in micro-, meso-, and nanoscales. Therefore it is not surprising that *chimie douce* sol-gel approaches [10] have gained much attention in chemical society [2, 15, 16] as the synthesis routes to complex oxide structures with well-defined and uniform crystal morphologies, surface area and pore size distribution, as well as in the coating applications [6, 17].

The first article, which can be considered as a report on sol-gel chemistry, was published in 1845 by Ebelman [10, 18], where he described the formation

of silica gels in ethanol from silicon tetrachloride at relatively low temperature. Although he did not use the term *sol-gel* in his report, he described the phenomena where colloidal particles form inorganic networks in liquid (sol) and the gelation of the sol where all the particles were connected to the network in a continuous liquid phase (gel) [10, 18]. With this work, conscious investigations of sol-gel chemistry have started, but it took almost hundred years to introduce the sol-gel method in industrial applications by Geffcken and Berger (1930) [19]. They used metal-containing precursors to coat industrial glasses with thin SiO₂ and TiO₂ layers. Encouraged by their success, several research groups continued to work on that new branch of chemistry with a view to develop entire new generations of advanced materials via sol-gel route. Although those investigations were rather episodic without receiving much attention, since then the coating of materials with thin layers in order to modify their surfaces has become and remained one of the major applications of sol-gel chemistry. Despite the success of this method in the coating applications, it did not gain any special attention among researchers and industrialists until 1970s, when Dislich [20–23] earned worldwide attention of scientists by synthesising transparent borosilicate glass from oxide powders by heating them at low temperatures. The oxide powders were obtained from a starting solution of ethanol, pentadiol, Si(OCH₃)₄, Al(O-secC₄H₉)₃, NaOCH₃ and KOCH₃ and heating post-synthesised gel pieces at 530 °C to transform them into oxide powder. After hot-pressing of the obtained oxide pieces at 630 °C, glass plates with properties very similar to those produced by the conventional melt-quenching technique were obtained [20]. It can be regarded as a new dawn of sol-gel process and the pioneering work on the synthesis of freestanding sol-gel structures besides coatings, that has been the main applications of sol-gel method so far. In those days the first attempts were made to prepare silica fibers for optical communication applications as well. Afterwards, scientists have never lost their interest on this method. However, despite promising discoveries, the sol-gel method attracted considerable scientific and industrial interest only over the past few decades, starting in the mid 1980's, when larger scientific community was caught by the research on nonhydrolytic preparation routes of mixed metal oxides (e.g., ZrTiO₄) [10, 24–27]. Enormously growing interest in this method is supported by the fact that the number of sol-gel-related publications per year has increased exponentially over the past 30 years (Figure 1). Despite the success of so-called non-hydrolytic sol-gel route, where metal halides are reacted with secondary or tertiary ethers as the oxygen source, the traditional or aqueous sol-gel route has maintained its position as a wet chemical method in the preparation of ceramic structures. Throughout the entire research of sol-gel method, it has been particularly successful in the synthesis of bulk metal oxides, like glasses, ceramics, fibers and films [10]. Therefore, thanks to the success of sol-gel method in mentioned fields in the past decade, this method has also been widely applied for nanoparticle synthesis [2, 15, 16]. One can even say that it has rooted as one of the main bottom-up synthesis method in micro- and nanotechnology in general.

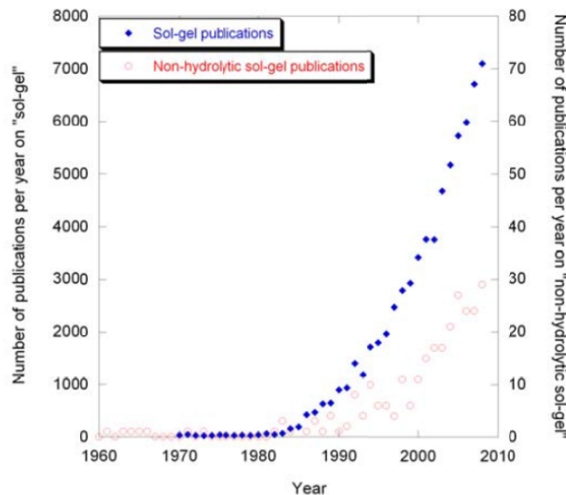


Figure 1. Number of publications per year on *sol-gel* [5].

The main reasons why the sol-gel method has become so popular, are mild preparation conditions (low temperature, liquid precursors) and characteristics of materials that can be produced without complicated instruments, compared with, for example, chemical vapour deposition (CVD) [28–32]. It overcomes the difficulties of producing materials with desired shapes, such as monoliths, films, fibers, powders [10, 11, 26, 33–36] and converting them into a ceramic material by annealing at temperatures that are much lower compared with those used in conventional sintering processes. When high purity, homogeneity, agglomerate free powders, narrow particle-size distribution, chemical durability, thermal resistance, are needed, the sol-gel process is probably one of the best choices [2, 6, 37–39]. To date, however, few if any sol-gel derived products are commercially available, in spite of a great number of articles published in journals. The reasons for this are manifold. It is widely believed that sol-gel products are either too expensive or lacking structural integrity, to be competitive with products obtained applying conventional ceramic routes [5]. Poor structural integrity may be caused by the deficiencies in some steps of preparation procedures of the sol-gel method which determines the materials texture. The stress evolution and crack formation are the representative drawbacks. In recent years, however, scientists have made a significant breakthrough in the understanding of the chemical nature of selected precursors and reactions involved in the sol-gel chemistry [40, 41]. This allows one to choose the right chemical strategy for synthesising procedures, which determines the materials texture and cost/availability for the industry. Therefore, it becomes possible to obtain techniques that also suppress the stress evolution and, hence, the crack formation. Solving these scientific issues would make it possible to apply sol-gel method also in industrial scale.

3.2. Principles of sol-gel chemistry

The literature includes myriad of publications concerning sol-gel chemistry as a synthesis technique in the fabrication of oxide materials [10, 42–59]. However, the question arises, whether the descriptions discussed in those articles strictly follow the definition of *sol-gel*. It can be seen that often the transformation of the molecular precursor to the dense bulk oxide does not exclusively proceed along the formation of the *sol* (nanohomogeneous colloidal system in liquid phase) and its subsequent transformation to *gel* (structured nanohomogeneous colloidal system in liquid phase) as a result of formation of chemical bonds between the particles, as it would be expected, when using the term *sol-gel* where „-“ marks equilibrium between the sol and gel forms of matter [10]. However, most of scientists have agreed that processes can be denoted as *sol-gel* as long as they include *sol* or *gel* as an intermediate stage and the transformation of the molecular precursor into the final solid compound involves chemical reactions in liquid phase under mild reaction conditions [10, 14, 19, 20]. On the basis of aforementioned terms, we can divide the entire process into following sequential operations including both chemical reactions and physical processes (phase separation, dissolution, evaporation, phase transition etc.)(Figure 2):

- Preparation of molecular precursor solution
- Conversion (polycondensation) of activated molecular precursors into sol (nanoclusters in solution)
- Gelation
- Aging
- Drying
- Sintering

In reality, the first two steps would occur practically in parallel, i.e. the condensation process begins before the hydrolysis is completed, and therefore the steps can hardly be distinguished. In spite of this, following these sequential or partially overlapping steps leads to the formation of solid material from liquid molecular solutions. A lot of reviews and books have been written, extensively describing and analyzing the general principles and physico-chemical bases of these steps [10, 42–59]. However, as it turns out, these principles, in particular the understanding of the mechanisms of hydrolysis and polycondensation, are changed over time, and are not equally applicable to silicon and the metal alkoxides. To bring out the main differences between the chemistry of silicon and metal alkoxides, a brief overview of those principles will be given below.

3.3. Chemistry of sol-gel processing

Sol-gel chemistry can be roughly divided into two different major routes - aqueous and nonaqueous sol-gel processes – depending on whether the precursor solution is an aqueous solution of an inorganic salt or an alkoxide, respectively [10, 60]. In the aqueous sol-gel process, the transformation of a

precursor solution into an inorganic solid via inorganic polymerization is induced by water. In contrast to that, in the case of nonaqueous sol-gel process, as the name implies, the transformation of the precursor occurs in an organic solvent under exclusion of water, and usually at slightly elevated temperatures. Despite these differences in the process, an oxide material is obtained via polymerization reaction by starting from molecular precursor solutions. Since these reactions take place in solutions, and in most cases near room temperature, i.e. at the mild conditions, the term *sol-gel processing* generally refers to the synthesis of inorganic oxide material by *wet chemistry* methods. To date, there has been synthesized wide varieties of different materials by sol-gel processing, the majority of which are transition metal oxides, from which the IROX™ TiO₂ film on glass, produced by Schott Glaswerke, is one of the most successful [61, 62]. However, the first materials synthesized by sol-gel process were silica-based, as pointed out in the chapter *History of sol-gel*.

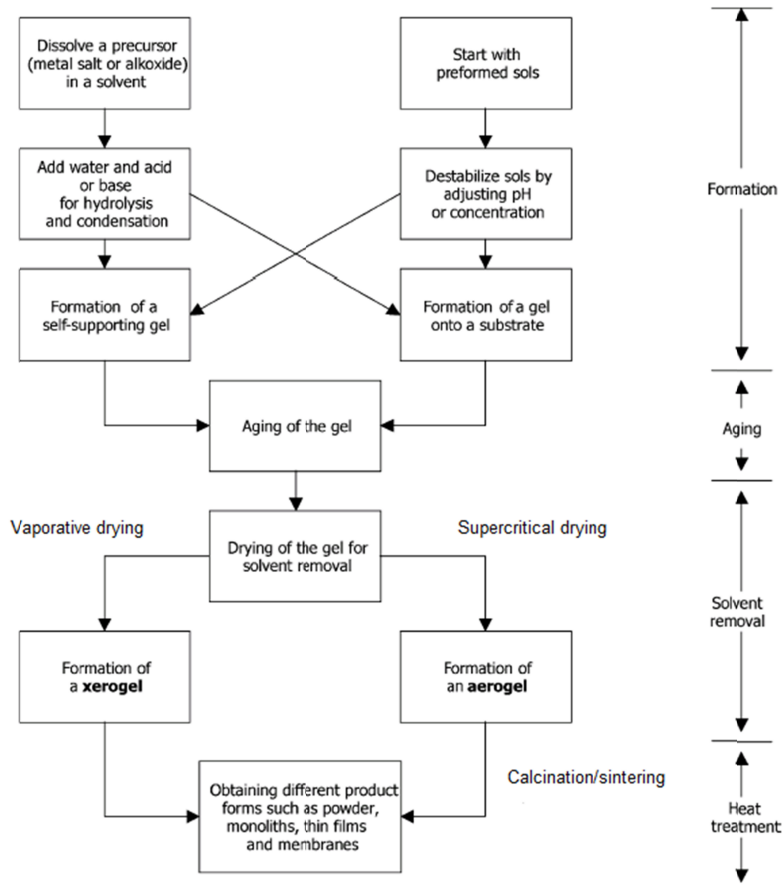
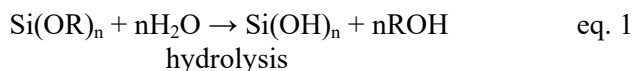


Figure 2. Steps of sol-gel chemistry [11].

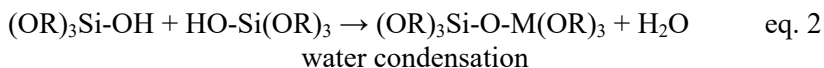
sol-gel chemistry. Silicon tetraethoxide (or tetraethoxysilane, or tetraethyl ortosilicate, TEOS – Si(OC₂H₅)₄) and silicon tetramethoxysilane (TMOS – Si(OCH₃)₄), namely, are the most studied examples. Thus, silica-based solutions have historically been the most widely used precursors in the studies on processing and synthesis principles of sol-gel materials. Those principles are later transferred to alkoxides in general, whether they are silicon alkoxides or metal alkoxides.

Further, we will look closer to those historically rooted synthesis principles of sol-gel chemistry based on the kinetically independent hydrolysis and condensation of molecular precursors, paying particular attention to the alkoxides as the most versatile precursor solutions in the sol-gel synthesis of oxide materials. Alkoxides are considered as compounds, which have an organic moiety (-OR) attached to a metal (M) atom through oxygen atom [63]. The metal atom is highly attractive to nucleophilic attack due to the electronegative alkoxy groups (-OR, hard π -donors) that stabilize metal atom in its highest oxidation state. Therefore alkoxides are very reactive with water, which leads to the formation of hydroxides or hydrous oxides. In general, the reaction can be written as:

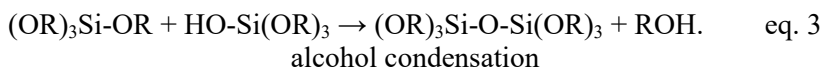


In the literature, the hydrolysis of the alkoxide is described as a nucleophilic attack of a water molecule to the positively charged metal or metalloid atom (M). As a result of that, the more easily leaving group, which is the alcohol, leaves (Equation 3) [64]. Hydrolysis ends when the amount of water is sufficient to replace all of the OR groups with the OH groups. Otherwise the metal or metalloid will remain only partially hydrolyzed, Si(OR)_{4-n}(OH)_n.

In condensation reaction, two partially hydrolyzed molecules can link together as follows:



or



Often hydrolysis and condensation reactions occur simultaneously and are hard to distinguish. In the case of silicon alkoxides, however, the condensation/polycondensation reactions are kinetically independent from the hydrolysis reaction. According to the widespread perception, the condensation reaction can follow one of the three pathways – oxolation, alkoxolation and ololation [65]. Condensation, by the definition, liberates a molecule of water or alcohol. This phenomenon is

attributed to the formation of larger molecules via polymerization process. A polymer (*many member*), or sometimes also called a macromolecule, is a big molecule formed from hundreds or thousands of monomers. Sometimes a word *oligomer* is also used. It refers to a molecule that has intermediate size i.e. is much bigger than *mono*, but much smaller than *macro*. Molecules can be either linear chains or strongly branched. It depends on how many bonds the monomer can form. The number of bonds that the monomer is capable to form, is called *functionality*, f . Monomers are commonly polyfunctional (bifunctional: $f = 2$, trifunctional: $f = 3$, tetrafunctional: $f = 4$). If an atom, for example Si, has two unreactive R groups and two reactive hydroxyl groups, $\text{SiR}_2(\text{OH})_2$, then this compound can polymerize into linear chains or rings only. But, if $f > 2$, a branched three-dimensional network can form. A *polymer*, however, is not a rigorous definition. According to Flory [66], the term *polymer* can be attributed to the structures with random branching. Hence, the definition could not be extended to crystalline solids. At first sight, still, the definition may be ambiguous. For instance, one can question whether an oxide glass, which is noncrystalline, is a polymer or not. To eliminate this ambiguity it is agreed that the average size of the closed loops constituting the network has to exceed significantly the atomic size.

Flory [64, 65] and Rabinovich [66] have introduced a term *particulate* in describing sols where nonpolymeric solid particles are dispersed into liquid phase. Later, Brinker and Scherer [67, 69] adopted the term to distinguish the particulate silica sols formed in *aqueous* solutions from the *polymeric* silica sols formed by hydrolysis of alkoxides in *nonaqueous* solutions. When extreme conditions (high pH) are excluded, silica-based sols show rather polymeric nature during gelation, whereas metal alkoxides prefer to form particulate sols [70]. In some cases the diameter of particles is in the order of 1 nm (*oligomers*), i.e. far from the size of the particles of polymeric silicates. Therefore, according to the definition of polymeric sol, proposed by Brinker, the solid phase contains no dense particles bigger than 1 nm – approximately the lower limit of the colloidal range [71]. Thus we can define particulate system as a system containing dense primary particles with the size over 1 nm.

Particulate sols can also form three-dimensional networks, when the dispersion forces get strong enough to stick the particles together. Unlike polymeric gels which are covalently linked (permanently), particulate gels are linked by van der Waals forces (reversibly). In real systems, condensation does not stop in the gel point. Further condensation takes place because the segments of the gel can still move, causing new bond-forming between different segments. In addition to that, liquid phase entrapped to the network still contains a sol with smaller particles that join the network.

Reaction kinetics of hydrolysis and condensation have been studied in number of works [72–85]. In the case of silicon alkoxides, the hydrolysis reaction is kinetically independent from condensation/polycondensation reaction. There are three competitive pathways for the silicone-based compounds following the condensation/polycondensation reaction – oxolation, alkoxolation and ololation

[84]. The kinetics is determined by the electronegativity of metal or metalloid atom. It is a well known fact that the transition metal alkoxides react very rapidly with water, even with the atmospheric humidity, as soon as they are brought into contact. Reaction times for metal alkoxides are 10^5 – 10^8 times faster than for silicon alkoxides [87]. Silicon alkoxides, on the other hand, are not very reactive with water. This is also the reason why the hydrolysis of silicon alkoxides requires catalysts for efficient gelation rates. The hydrolysis can be catalyzed either by acids (HCl, HNO₃, H₂SO₄) or by basis (NaOH, amines), as shown in figure 3. The following reactions are different in terms of the mechanism and kinetics, resulting in the first case with the formation of rather linear polymers via S_N1 nucleophilic substitution mechanism and in the second case usually with highly cross-linked aggregates via S_N2 mechanism. The latter stems from the fact that the base catalyzed S_N2-type process makes the partially hydrolyzed silicone alkoxide species more prone for further hydrolysis than condensation. Therefore, generated monomeric particles are able to link together and form three-dimensional aggregates. Despite this, cross-linking of linear, acid-catalyzed chains, is also possible by interlinking of chains. In the case of base-catalyzed systems, the cross-linking starts at the beginning of the process. Thereby it is very important to consider the water to alkoxide ratio (R-value), which influences the structural evolution of the material being prepared. More precisely, it determines the size of forming particles and the degree of cross-linking.

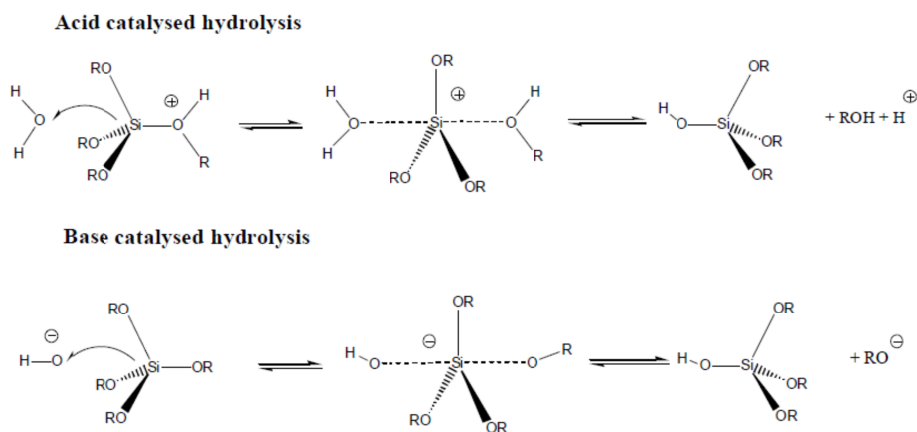


Figure 3. Differences between acid and base catalyzed hydrolysis [66].

Unstability of transition metal alkoxides toward hydrolysis is explained with the partial positive charge which is much higher for transition metal alkoxides compared with that of silicon. Approximate estimation of the partial charge distributions of some alkoxides are shown in table 1. According to this, metal

alkoxides must be handled very carefully. Often stabilizing agents are added to the alkoxides in the sol-gel process [15, 88].

Table 1: Positive partial charge of M for ethoxides.

| Alkoxide | Zr(OEt) ₄ | Ti(OEt) ₄ | Nb(OEt) ₄ | Ta(OEt) ₄ | W(OEt) ₄ | Si(OEt) ₄ |
|----------|----------------------|----------------------|----------------------|----------------------|---------------------|----------------------|
| δ(M) | +0,65 | +0,63 | +0,53 | +0,49 | +0,43 | +0,32 |

Reaction kinetics is also influenced by the oligomerization (molecular complexity) of the metal alkoxides. It depends merely on the nature of particular metal atom. In the group, the complexity increases with the atomic size of the metal (Table 2). This explains why the divalent transition metal alkoxides (Cu, Fe, Ni, Co, Mn) changes insoluble as a result of polymerization [89, 90]. A good example of the molecular complexity is the formation of precipitate from Zr(OPrⁿ)₄, dissolved in polar solvent, n-PrOH, whereas, if dissolved in nonpolar solvent, the precipitation can be avoided. On the other hand, reaction kinetics is also influenced by the characteristics (size, electron providing) of organic ligand. For example, the length of alkyl chain of titanium n-alkoxides, Ti(ORⁿ)₄, affects the reaction rate. Decrease of the chain length decreases also the reaction rate [91–93].

Table 2: Molecular complexity (number of metal atoms per osmotic molecule) of some transition metal ethoxides as a function of metal atom size.

| Compound | Ti(OEt) ₄ | Zr(OEt) ₄ | Hf(OEt) ₄ | Th(OEt) ₄ |
|----------------------|----------------------|----------------------|----------------------|----------------------|
| Covalent radii (Å) | 1,32 | 1,45 | 1,44 | 1,55 |
| Molecular complexity | 2,9 | 3,6 | 3,6 | 6,0 |

The size of the forming molecule depends how many bonds the monomer of alkoxide can form by hydrolysis. If it is more than two, then there is no limit on the size of the molecule. The growth of the molecule may end with the gelling point i.e. when the dimensions of the macroscopic molecule extend throughout solution.

3.4. Transition metal oxides

Transition metal alkoxides, M(OR)_n, are the most widely used molecular precursors in sol-gel processing [6, 84, 94–101]. Their popularity stems from the circumstances that they are usually easily accessible and inexpensive and easily converted to oxides. The last feature makes them in the eyes of chemists more desirable precursor candidates than, for example, inorganic salts (sulfates, chlorides, nitrates). Recent works in the field of sol-gel technology, including

studies on both molecular and crystal structure and the reactivity of these compounds, have considerably changed the understanding of chemical nature of alkoxides, in the eyes of both chemists and materials scientists. It turned out that the compounds earlier considered to be $M(OR)_n$ are in fact oxoalkoxides $MO_x(OR)_y$ [40, 41]. Due to the formation of a large number of oligomeric species, which depends on the oxidation state, on the pH or on the concentration, the chemistry of transition metal salts can be rather complicated. The metal ions are coordinated by the counter anions. Just as the removal of these anions from the resulting product may be quite a challenge, they can also influence the morphology, the structure and in the some cases even the chemical composition of the final material [10]. Therefore, many of these problems can be avoided by the exploitation of metal alkoxides as precursor solutions, instead of salts. Another major issue associated with sol-gel chemistry based on the hydrolysis and condensation of molecular solutions, is the control over the reaction rates. Based on the common understanding about the kinetics of sol-gel reactions, in particular the hydrolysis and condensation, which is based on the silicon alkoxides, these reactions are kinetically independent. For the majority of alkoxides, like transition metal alkoxides, however, these reactions occur too quickly, in other words, it is practically impossible to identify when the hydrolysis reaction ends and the condensation reaction starts. This inhibits morphological and structural control over the final oxide material. Furthermore, this makes it very difficult to control the composition and homogeneity of complex multimetal oxides, due to the different reactivities of metal alkoxides [10]. Therefore organic additives are used to decrease the reactivity of precursors. Additives like β -diketonates, functional alcohols and carboxylic acids act as chelating ligands and decrease their reactivity [10, 46, 100–110]. Any slight changes, even the smallest ones, in the synthesis parameters may lead the whole process to an undesirable final result. Taking into account also the hardly distinguishable hydrolysis and condensation reactions, it is almost impossible to fully control the sol-gel process.

Turova *et al.* [84] have pointed out in the review book „The Chemistry of Metal Alkoxides“ the main advantages of the sol-gel processing of alkoxides in order to obtain oxide materials as follows:

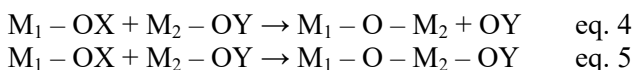
- majority of the alkoxides, $M(OR)_n$ ($n \leq 3$), are easily purified by the distillation or sublimation (below 200 °C) or by recrystallization from organic solvents;
- metal alkoxides are very prone to the hydrolysis reaction, forming intermediate reaction products – hydrated oxides that are free from any extra anions, in contrast to the precipitation method from the aqueous mixtures of inorganic salts;
- small agglomeration rate, very high hydration rate (minimal amounts of M-O-M bridges) and high reactivity of the forms $M_2O_n \cdot xH_2O$ makes them excellent candidates to form stable colloid systems – sols and gels;
- relatively low temperatures of dehydration of sols/gels that sometimes occurs during the hydrolysis reaction, forming very small oxide particles

possessing well-developed surfaces, high chemical activity and usually amorphous or metastable phases that can be transformed into more stable forms by the subsequent thermal treatment;

- metal alkoxides are usually pure, inexpensive and easily available for the synthesis of highly homogeneous oxide gels, glasses, fibers, films, etc.

Chemically, alkoxides are extremely weak as acids, easily removable via hydrolysis and thermal annealing, leaving highly pure hydrated solids. These features have made metal alkoxides the most common candidates of molecular precursors [11, 40, 41]. Titanium- and zirconium-based alkoxides are widely used for the preparation of glasses and ceramics. Metal alkoxides are known for their very high reactivity towards water and atmospheric humidity. Interaction with airborne water molecules or even poorly dried solvents results in extensive changes in molecular complexity and chemical composition [111–115].

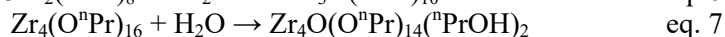
In metal alkoxides, metal atoms are stabilized in their highest oxidation states by the very electronegative OR groups. Therefore it is very important to handle the alkoxides with great care. There is a vast amount of literature available which describes the reactions of metal alkoxides. Although they are distinguished from silicon alkoxides, $\text{Si}(\text{OR})_4$, by several factors, like lower electronegativity and stable coordinations, still, as shown in the majority of articles, reactions with metal alkoxides are considered to proceed almost exclusively through the $\text{S}_{\text{N}}2$ type mechanism like in the case of non-metal, silicone alkoxides. It has been suggested in the literature, that metal alkoxides at first form hydroxo-alkoxide species like $\text{Ti}(\text{OR})_3(\text{OH})$ or $\text{Zr}(\text{OR})_3(\text{OH})$ as results of hydrolysis of alkoxide *monomers*. Formed species can then become further hydrolyzed or undergo condensation, which results in the formation of oxo- (oxolation) or hydroxo (hydroxolation) bridges [116]. In this case, the hydrolysis and condensation are viewed as two independent kinetic regimes (also referred as a two-step hydrolysis-condensation) like in the case of silicon alkoxides. Thereby, the condensation is handled as a polymeric condensation (polycondensation). In more detail, the condensation of transition metal alkoxides is proposed to occur *via* one of the two nucleophilic mechanisms: nucleophilic substitution (S_{N}) takes place when the preferred coordination of metal atom is satisfied and nucleophilic addition (A_{N}) occurs when the preferred condition is not satisfied:



In first case, a hydroxy bridge is formed between two metal centers [84]. This is called ololation. Alternatively, two metal centers are linked via *oxo* bridge (- O -). This is called oxolation.

Extremely rapid kinetics of metal alkoxides cause fundamental studies to be much more difficult than for silicon alkoxides. Recently, however, Kessler and Schubert [40, 41, 117–119] have persuasively demonstrated that the hypothesis

of kinetically controlled hydrolysis-polycondensation is insufficient to describe the sol-gel process of metal alkoxides. The main argument that supports this theory, is the fact that metal alkoxides are not monomers, like silicon alkoxides, but oligomers [40, 41]. Its due to extreme Lewis basicity of the alkoxide anions RO^- . If small amount of water is added to the metal alkoxides, then microhydrolysis does not end with any hydroxide intermediates. Instead of that, well-defined oligonuclear oxo-alkoxide species are formed directly through one-step hydrolysis-condensation transformation, which is caused by the restructuring of the precursor molecules, for example [40, 41]:



The parameter having the greatest impact on both silicon and metal alkoxide hydrolysis reactions is the molar ratio of reactants, also called the R-factor, in the literature often denoted also as a hydrolysis ratio h . It is defined as a ratio of water molecules to metal alkoxide molecules ($R = [\text{H}_2\text{O}]/[\text{M}(\text{OR})_n]$) [84]. Proper ratio allows one to achieve the formation of material with distinct structure. It is also shown that the obtained metal alkoxide species have extremely complicated structures (Figure 4). Kessler [40, 41] has compared the molecular structures of the individual hydrolysis products of metal alkoxides with the structures of well known oligonuclear inorganic oxometallates (M_3O_{11} , M_4O_{16} , M_6O_{19} , M_7O_{24}).

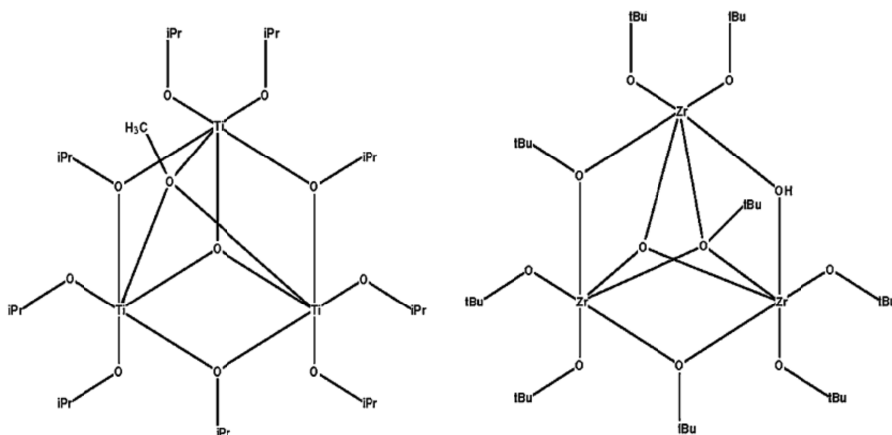


Figure 4. Molecular structures of the titanium [99] and zirconium [100] microhydrolysis products.

Mosset *et al.* [122] have shown that different hydrolysis ratio results in different almost spherical aggregates. For the titanium ethoxide, for instance, different conditions for partial hydrolysis, i.e. different hydrolysis ratios, have also resulted with such aggregates as $\text{Ti}_8\text{O}_6(\text{OEt})_{20}$ [123], $\text{Ti}_{10}\text{O}_8(\text{OEt})_{24}$ [124] and

$\text{Ti}_{16}\text{O}_{16}(\text{OEt})_{32}$ [122]. Although the hydrolysis ratio is the most decisive factor, considering the progress of microhydrolysis, it also depends on the complexity of the solution and may be rather selective. In the case of more complex media, only one or few of the components are transformed into oxoalkoxide species, as a result of microhydrolysis and changing thereby the stoichiometry of molecular precursors. However, these undesirable phenomena can be avoided if all the operations in the preparation process, like weighting the alkoxides are carried out in dry atmosphere using a Schlenk line or a dry box and solvents dried with the reliable technique are used [84]. From the perspective of reproducibility of the process, strict control of the reaction temperature and stoichiometry is of crucial importance.

Recent studies have disproved also the effect of heteroligands to the hydrolysis and condensation kinetics. One of the main differences between metal alkoxides and silicon alkoxides is the high mobility of the ligands of metal alkoxide. It turned out that, in the case of metal alkoxides, heteroligands are easily transferred also between different molecules, not only within one molecule, as was believed so far. Moreover, they tend to be considerably smaller than the alkoxide ligands they can replace. For example, crystallographic studies have shown the size difference between the acetylacetonate (acac) ligand and ethoxide ligand, where the first one has the size of two ethoxide ligands [40, 41]. Two isopropoxide ligands, which can also be replaced, are even much bigger (Figure 5). The entire process of sol formation is related to the self-organization of the ligands, rather than to the kinetics of hydrolysis and polycondensation.

3.5. Formation of metal-oxo-nanoparticles

In the 1960s, Don Bradley [124] proposed the hypothesis for formation of densely packed molecular oxoalkoxide products by addition of substoichiometric amount of water to the alkoxide. Structure of mentioned primary particles was derived from the arrangement of cations and anions. Later it became clear that the stability of these primary particles is most likely determined by the interactions on its surface, which in turn depends on the absence of residual organic ligands. Recently, Kessler [40, 41] denoted these particles as Micelles Templated by Self-Assembly of Ligands (MTSAL). He also claimed that the size of particles depends on the conditions of coordination equilibrium and ligand-solvent interactions. The particle size will generally be in the range of 2–5 nm (Figure 6). Therefore, we are dealing with the particulate sols, which were described in the previous chapters. Single crystal X-ray analysis has proven that even the particle diameter is about 2 nm, it can still incorporate hundreds of metal atoms [125–129].

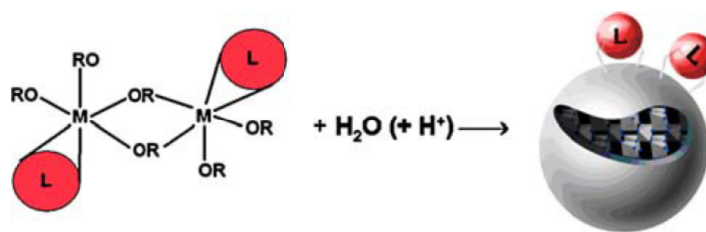


Figure 5. Formation of a Micelles Templated by Self-Assembly of Ligands (MTSAL) - primary particle of the sol-gel process. L stands for the ligand group. Kessler *et al.* [40, 41].

Consequently, two questions arise: how big can the particle grow and why is the size defined in so narrow range. The reasons are manifold: thermodynamic parameters (solubility of the oxides, diffusion coefficients of the cations) from one side and heterogeneous kinetic parameters on the other hand. Lundqvist and Persson have calculated, on example of titania, that particles with smaller diameters have higher activation energy [130, 131]. Therefore it can be assumed that the growth of the aggregate ends when it is not kinetically favorable, i.e. when a certain limiting size of aggregate is achieved. This theory has experimentally been proven by several groups of scientists. The further growth of particles is still possible, depending on the conditions of subsequent processing. Amorphous shell makes the particles reactive with each other and they can form bigger aggregates, when interacting to each other. There are two ways for the binding, either via formation of M-O-M bonds or via hydrogen bonding. The size of forming aggregate depends on the hydrolysis ratio and the presence of gelating ligands. At smaller ratios also smaller aggregates can form and, hence, uniform transparent sols and gels will occur. It is promoted by the strong interactions between ligands and solvent. At higher ratios, however, the aggregation of particles takes place in the entire volume range of the solvent, thereby, in the absence of ligands. In the latter case dense gels or precipitates will form. Further processes of MTSAL will be viewed in the following chapters.

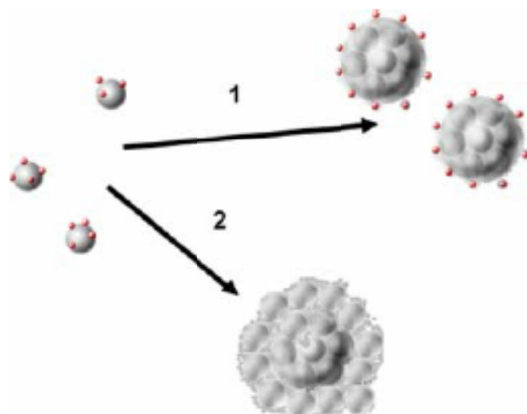


Figure 6. Aggregation of primary particles in case of low hydrolysis ratio. Essential amount of ligands interacting with the solvent ends with the formation of uniform transparent sols and gels (1). Higher hydrolysis ratio and absence of necessary ligands results in dense and non-uniform aggregated gels or precipitates (2). Kessler *et al.* [40, 41].

Almost analogous oxide and sulfide MTSAL primary particles, with the average size about 5 nm, have been also obtained by applying the non-hydrolytic sol-gel route of metal alkoxides [40, 41]. But in contrast to the hydrolytic process, in this case the obtained primary particles are fully crystallized. This difference is caused by the avoidance of dehydration process – the main drawback of the crystallization in the case of hydrolytic process.

3.2.1. Preparation of molecular precursor

The sol-gel process starts with the preparation of molecular precursor solution via dissolving metal-O-organic material in an organic solvent that is miscible with water or via dissolving inorganic salts in water [10, 11, 84]. The formation of a clear colloidal solution (*sol*), as a result of primary condensation (via hydrolysis) of dissolved molecular precursor, is the main peculiarity that makes the sol-gel technique unique and distinguishes it from other methods. This step is followed by the second peculiarity of sol-gel process – the formation of chains by chemical bonding of these colloidal particles [10, 36]. The cross-linking of the changes in to three-dimensional network as a result of ongoing chemical reactions is called *gelation*. The condensation reaction itself is caused by the local reactive groups on the surface of particles. In general, the gels can be considered as a stable colloidal systems where all ingredients and phases are equally distributed in the entire volume of the system. Or, alternatively, they can also be considered as colloids, consisted on solid matrix, where the spaces around its knots are filled by liquid [132, 133]. This transformation, from sol to

gel, is called the sol-gel transition (hence the name *sol-gel method*). The gelation competes with the process of flocculation- a process wherein colloidal particles precipitate from the suspension in the form of floc or flake. This process is caused by the isotropic micelle aggregation (Figure 7). Previously described stages are both controlled by the condensation chemistry that can include either hydrolysis of hydrated metal ions or metal alkoxide molecules as a first step [36, 105, 116, 134]. The condensation chemistry itself is based on the reactions of olation/oxolation between hydroxylated species [36, 105, 116]. Further, there are two possibilities to dry the obtained gels, which divide the materials obtained into two general categories: xerogels and aerogels [5]. Removing the pore liquid under ambient conditions causes shrinkage of the pores and yields with the xerogel. Another opportunity is the removal of the liquid from the network under hypercritical conditions. In this case the network does not collapse due to missing of liquid-gas interface which leads to aerogels – an ultralight materials with extremely low density [10].

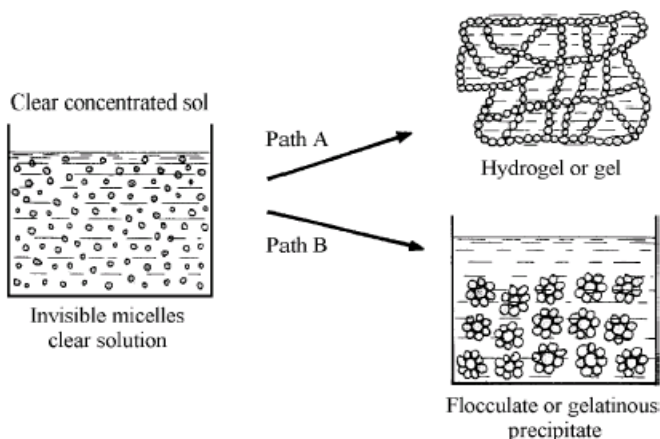


Figure 7. Formation of gel versus flocculates [84].

Sol-gel method, like any other, have also some deficiencies, which should be specifically taken into account during the process in order to prevent undesirable course of reaction. The first drawback comes with the precursor solutions if the metal alkoxides are applied as the starting reagents [91]. Due to their extremely high sensitivity to water they commonly lead to formation of a precipitate [4, 6, 135–140]. Inhomogeneous precipitation during sol-gel processing is usually an undesirable phenomenon that scientists are trying to avoid, searching for the most optimal reaction parameters (hydrolysis and condensation rate of the molecular precursors, temperature, pH, mixing, rate of oxidation). Unfortunately, such a vast number of parameters that need to be strictly controlled, in order to provide good reproducibility of the synthesis, makes the sol-gel processing difficult to control [10, 34].

3.2.2. Aging

Process following to the gelation is usually aging. As it was mentioned above, the formation of solid, three-dimensional network does not stop completely in the gel-point. Aging is the process where the solid network continues to evolve. It involves three steps: continuing linking of particles with each other, syneresis and coarsening. During the first step, unlinked primary sol particles, still absent in the liquid phase, will join into the solid network. This step ends when all of the free particles are networked. At the same time, the material shrinks. Next step – syneresis – is a spontaneous and irreversible shrinkage of the material. Result of this process is the expulsion of pore liquid. This is also the source of stresses. The expulsion of pore liquid follows the Darcy's law [11, 141], whereby the flux J is proportional to the gradient of the liquid pressure:

$$J = -\frac{D}{\eta_L} \nabla P_L,$$

where η_L is the liquid viscosity and D is the permeability of the liquid. The last step – coarsening – also referred to as Ostwald ripening, comprises dissolution and reprecipitation. In this process surfaces with different radii of curvature play an important role, thereby setting off differences in solubility. During coarsening the strengthening of the gel takes place, without any shrinkage. The process depends strongly on the temperature, pH, concentration and type of solvent [11].

3.2.3. Drying

As described above, sol-gel preparation of bulk oxide structures includes the gel formation, aging, drying of gels and subsequent annealing of the gels to get dense oxides [66]. Drying of an as-synthesized gels is one of the most critical processes. One can even say that it is the major obstacle in producing bulk, unbroken sol-gel-derived structures (films, fibers, tubes). It's due to the fact that as-synthesized gels are wet, i.e. the pores of material are filled with residual liquid phase. Liquid phase entrapped in the pores are the main reason of cracks and fracture of the material during drying process. Therefore, understanding even the smallest nuances of this part of the sol-gel process is crucial to obtain unbroken structures. The methods for avoiding that usually undesirable phenomenon are also thoroughly described by Sakka et al. in the *Sol Gel Processing* [11].

The exact amount of residual solvent left to the gel depends on the processing conditions. After drying, obtained xerogels contain 40–75 vol.% pores, from which it can be concluded that the amount of liquid phase in gels are rather high [84]. Pores occur if the gaps are left between connected particles or networks of the material. At the first stage, the whole gel body is covered with liquid phase which then enter into the surface layers of the gel body. The best

theory so far, which describes that phenomena, is provided by Zarzycki et al. [11, 142]. In their considerations the cracks occur in drying gels when the capillary forces exerted by the pore liquid to the pore wall exceed the strength of the gel network. This theory regards the fine pores as capillaries with the diameter D . At the menisci, the solvent with surface tension γ causes the capillary force ΔP :

$$\Delta P = \frac{4\gamma \cos\theta}{D},$$

where Θ is contact angle between the solvent and capillary wall. The resulting pressure generated is proportional to the specific surface energy at the liquid-air interface. During the drying process most of the residual solvents are vaporized from the pores of surface layer of gel, thereby causing the shrinkage of this layer. However, since the inner layer of the material does not shrink, it generates the tensile stress in the surface layer. By the Zarzycki *et al.* [142], this results in the crack formation or fracture if the stress exceeds the strength of the gel. For example, if a pore with the radius of 2 nm is filled with water, the pressure may reach 73 MPa, assuming that the wetting of the liquid is perfect (Figure 8). The solution for this problem might be an application of long drying times, i.e. the evaporation rate of the liquid should be very low. But in practice this is still not an applicable solution because of too long process times, reaching even months or years to form a monolithic xerogels. Instead of that, surface tension of the liquid can be modified by adding drying control chemical additives (DCCA), like formamide [11, 84, 143].

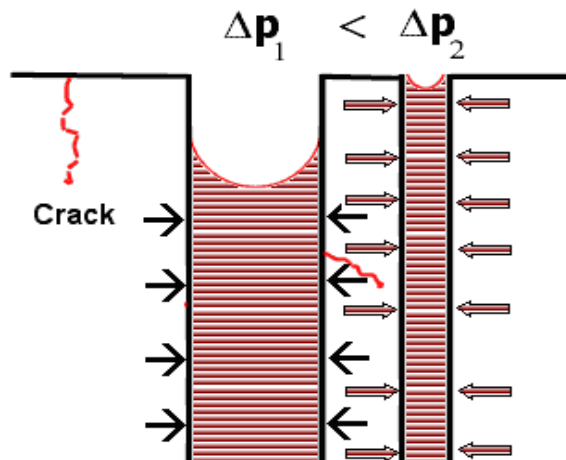


Figure 8. Crack formation in sol-gel derived metal oxide materials [23].

Another technique, developed by Kistler [144, 145], to prevent crack formation during drying, is to dry the gels in an autoclave under supercritical conditions. However, it should be noted that the path of the thermal treatment and the equilibrium curve do not cross. This technique was successfully implemented by Nicolaon and Teichner [146] to gels obtained from metalorganic compounds. Montpellier developed the supercritical technique by the systematic investigation of optimal parameters of the drying process [11, 84]. The critical point can be bypassed by two different ways: addition of some extra liquid in to autoclave and heating or by applying pressure of the inert gas before heating, but in either case the resulting material is highly porous. This very unusual, highly porous product, where pores are filled with air, is called aerogel. Several papers are devoted to aerogels [147–153].

3.2.4. Thermal treatment

Near-room-temperature synthesis, which is one of the advantages of sol-gel method, on the other hand, leads to a problem, in many cases the materials are needed in chrystalline form, which for they are to be heat treated. In order to obtain crystalline oxide materials, the xerogels require post-synthetic thermal treatment, to induce the crystallization process. However, the common sintering temperatures of sol-gel materials still remain below the sintering temperatures of the conventional powder-ceramics. Control over crystal size and shape during this step, however, are obstructed. This limitation plays only a minor role in the case of synthesis of bulk metal oxide materials, contrary to the synthesis of nanoparticles, where they represent the major issue [10]. In addition to that, thermal treatment of as-synthesized structures generates stresses inside the material which are the origins of the cracks. Although most of the residual solvent entrapped in the as-synthesized gels are vaporized from the pores during drying process, small amount, nevertheless, remains inside the pores after drying. During the heating of the gels, solvents have to be removed and at the same time, sintering of the material has to take place. Thus we can say that pores play an important role in forming crack-free structures.

During the heating procedure, gel structures experience following stages: heating-up, isothermal heating (annealing), and cooling-down. In the first two stages, gel structures undergo significant changes in structural composition and chemistry. This transformation results with the evolution of stress. Stress that occurs at the stages of heating-up or annealing, is called *intrinsic stress* [11].

The stress generation and the crack formation in the heating-up stage could also be caused by the densification behavior of gel structures, which are likely affected by a number of processing parameters. The extent of hydrolysis (H_2O /alkoxide molar ratio) of precursor solution, i.e. the amount of water for precursor hydrolysis, is one of the factors. In order to know the effect of water, *in situ* stress measurements have been carried out by Kozuka [154]. Although silica gel films deposited on single-crystal Si substrates were applied in the

latter study, it likely describes the stress evolution and crack formation in the metal alkoxide-derived gels as well. The nature of this stress is tensile and increases with temperature. Experimental results indicate that higher hydrolysis ratios cause higher stress. It can be explained with the larger extent of polycondensation reaction occurring in the material during heating. This, in turn, is caused by the larger amount of the OH groups susceptible to polycondensation reaction. In other words, the higher stress at higher hydrolysis ratio is caused by the higher capillary pressure [11].

As mentioned above, the crack formation is always observed on planar gel films deposited on some kind of a substrate. Thus, probably the main reason for cracking in such cases is the difference in the thermal expansion coefficient of the observed gel film and the substrate material. Consequently, it can be assumed that in the case of freestanding gel structures (fibers, tubes etc.) the origin of the cracks lies in the pores only. SEM images taken earlier [11, 84] show, that these microcracks emerge along grain boundaries, which means that they are formed after crystallization.

Even if the microscopic cracks do not affect the integrity of the sol-gel structures, then the macroscopic cracking becomes fatal to those structures, leaving only small pieces of the initial gel body. Unfortunately, there are only few researches discussing that significant problem, and only couple of these studies include the *in situ* investigations of macro-cracking. Brinker et al. [15, 29, 42] have proposed a theory on the macrocrack formation. According to them, the macroscopic cracking is caused most likely due to the intrinsic stress (not due to the thermal stress, which develops in the cooling stage) in the heating-up stage. However, since the observations were always done after the thermal treatment, it is only hypothesis, which has not been confirmed experimentally. So, according to this study, the question still remains; in which thermal treatment stage, i.e., the heating-up, annealing, or cooling-down stage, the gel structures crack and decompose.

In situ investigations of macroscopic crack formation have shown that the cracking does occur in the heating-up stage at 100–400 °C as a function of heating rate and film thickness (can be considered also as a thickness of all kinds of freestanding structures). Observations on titania films have shown that macroscopic crack formation have occurred at temperatures lower than 500 °C, which is the crystallization temperature of titania. In other words, cracks occurred prior to crystallization. Therefore, it can be concluded, that the macroscopic cracking is caused by the tensile stress due to the densification of the material in the heating-up stage, not due to the thermal stress in the cooling-down stage.

The experimental results indicate that at the lower heating rates cracking occurs at the lower temperatures, as shown in Figure 8, where the cracking is plotted as a function of heating rate. Simultaneously, lower heating rate results in lower porosities, which means that material has more time to be densified during the heating-up stage.

It is a very well known fact that thicker films are more eager to crack macroscopically than thinner films. Effect of thickness to the crack formation during the thermal treatment has been investigated by Kozuka in a number of works [154–158]. A series of films from silica and titania gels was prepared with various thicknesses by spin-coating. These studies revealed that the cracks were formed in thicker films at lower temperatures, as can be seen in Figures 12–13. However, there is no information available about how the intrinsic stress generated in the heating-up stage is affected by the thickness of the film.

Garino [159] has studied how the amount of water for microhydrolysis ($\text{H}_2\text{O}/\text{alkoxide}$ ration) affect the cracking-onset-temperature of films. According to his report which comprises alkoxide-derived silica films, increasing the hydrolysis ratio decreases the critical cracking thickness. Higher hydrolysis ratio causes higher stress in the film and is thus related to the lower cracking temperature. In contrast to that, the cracking temperature of the thinner films is higher.

In the case of more crystalline materials and due to the nanoparticulate structure, the cracks may differ in the way of propagation and the shape. At the lower temperatures they tend to propagate curled and at higher temperatures likely straight [11, 84, 159]. This phenomenon may be caused by the increase of the stiffness of the gel film during the increase of heating temperature. Increase of the stiffness takes place as a result of polycondensation reaction and densification. This type of the process of course would make the material brittle, allowing therefore propagation of straight cracks. At lower temperature, however, the development of the three-dimensional network is not yet finished and therefore the material maintains its plasticity. In this kind of material the way of crack propagation is not strictly determined, leading to cracks with arbitrary shape.

In sol-gel processing the humidity of surrounding atmosphere and chemical composition of precursor material also play important roles and affect the onset temperature of cracking. As can be seen in the Figure 12–17, where the cracking temperature is plotted against the humidity, increasing relative humidity will decrease the cracking temperature. In other words, when the gel structures are obtained and annealed at higher relative humidities, cracking of the material can take place at lower temperatures. Reason for this phenomenon has not yet been found out, but there is a couple of theories: water vapor may cause the post-hydrolysis on the surface of the gel structure, inducing solidification of the surface and, thereby, leading to the increase of stress gradient across the thickness; the capillary pressure in the material may be increased by the adsorption of water molecules on the surface of the gel structure, increasing thereby the tensile stress.

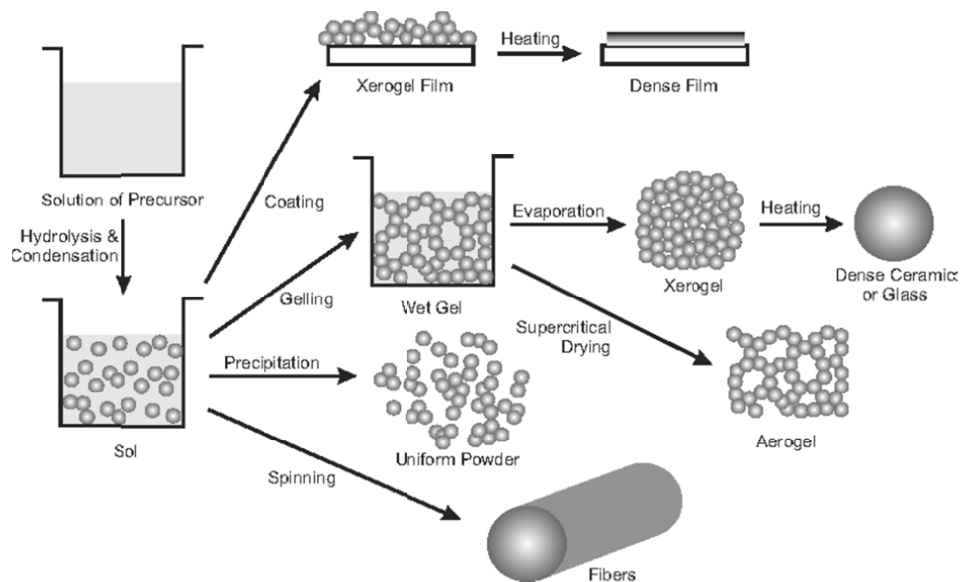


Figure 9. Main steps of sol-gel processing for preparation of different shape inorganic gel materials [10].

3.6. Microtubes

Several methods are proposed as a prior art for preparation of 3D ceramic micro-materials including microtubes. One of the methods, widely applied for the preparation of micro tubular ceramic materials, is based on using organic or anorganic fibres, different membranes, ionic liquids etc. as templates [160–184]. These templates are covered by a layer of ceramic materials by using sol-gel technology [160–184], coating of the surfaces by different mixtures of ceramic precursors [185], chemical vapour deposition (CVD) processes [186, 187], laser deposition processes [188], thermal vapour deposition [189] layer by layer adsorption coating [183, 184], electrophoretic deposition [190], hydrothermal deposition [191] or some other methods. The tubes are obtained when the template at the core of these structures is removed. This can be done by using burning, melting or dissolving of the template (Figure 10). The weakness of the method is that it enables preparing of materials with low structural homogeneity. The size and shape of the pores inside the final material depends on coating procedure, diameter of the template fibre, thickness of the ceramic coating on template and on the coating method. As the removal of template could cause changes of its volume, inhomogeneities and cracks could appear during the processing. Expensive technologies are needed when ceramic layer is carried onto the surface of template by using CVD, atomic layer deposition, laser deposition or thermal vapour deposition. Due to the unhomogeneous

structure of the tubes obtained by template method they can only withstand 2–3 atm pressure differences applied between the inside and outside of the tubes.

Another known method for the preparation of ceramic tubes is extrusion, which enables to prepare hollow ceramic materials by pressing viscous-elastic precursor materials into a suitable shape mold [192]. The tubes can also be prepared by pressing the precursor through a suitable shape nozzle. Solidification of precursor is achieved as a response to cooling, chemical reaction or chemical reaction caused by UV radiation [192, 193, 194]. Minimal dimensions of materials obtained by extrusion remain in the 1 mm range defined by the dimensions of the mold or nozzle. The obtained fresh tubes are sintered at elevated temperatures to increase their density, to remove the additives and to increase the strength and hardness of the material. Extrusion is the most widely applied top-down approach for preparation of metal oxide ceramic materials in form of tubes and fibres. It is cheap to apply the technology in microscale. However, the method can not be applied for the preparation of microtubes, which have an inner diameter below 100 μm because, in addition of miniature nozzles (diameter 100–1000 μm), advanced precursors are also required. For that, the precursor should be homogeneous in nanoscale containing no particles bigger than 1–2 μm . Moreover, the precursors should possess suitable viscous-elastic properties to avoid the collapse of freshly extruded structures under the high surface energy of the precursor. All those requirements make the method too expensive for the production of tubes in microscale. A disadvantage of the method is that freshly pressed tubes are soft and difficult to handle in further processing [192].

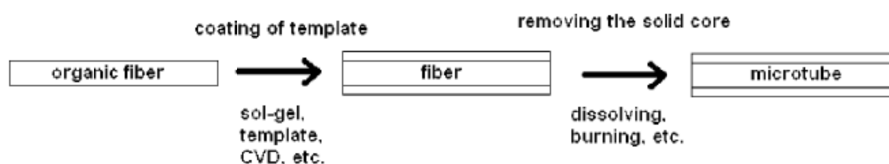


Figure 10. Template method for microtube fabrication.

Metal oxide microtubes can be milled out from larger size monoliths. It can be done by cutting mechanically or by using an electron or ion-source. This method enables preparing the tubes made of almost all metal oxide materials including their very hard monocrystalline forms. The drawback of the method is its costly nature as exact mechanics and cutting tools.

The method to build up the tubes atom by atom or molecule by molecule as a result of self-formation processes is known as bottom-up approach for materials preparation. The tubes form as energetically the most favoured structures. Diameter of the tubes is defined by size of catalysing particles. The method is suitable for preparation of very small nanotubes in diameter range from 1 to 100 nm. The formation of tubes with a bigger diameter is energetically unfavoured

as growth remains too low and the number of defects in the tube structure increases.

Another widely known method for the preparation of tubes is based on roll-up of thin layers of materials. The suitable conditions have been suggested for the self-formation of metal oxide ceramic tubes in micro-scale. For that, the selected substrate is coated with a metal oxide precursor. The tubes can roll up when the substrate is removed, which can be done by dissolution or mechanical cleaving. The roll-up process is supported by the tendency of materials to minimize their surface energy [195–198]. The parameters (length, wall thickness, and diameter) of the tubes are controlled by the length and thickness of the initial film piece and the selection of solvents. A drawback of the method is that the tubes which form have an open edge, wherefore they can neither be applied for pumping liquids nor gasses under pressure.

Yet another known method for the preparation of different shape 3D ceramic structures, including microtubes, is microstereolithography [199]. This process is controlled by using a beam excitation with, e.g., a laser, and the structures are grown up layer by layer. The method is rather expensive as it requires high-precision mechanics. As the final structures are achieved by growing them layer by layer, the process is also time consuming.

The use of sol-gel technology in preparation of metal oxide ceramic microtubes is known as a part of prior art. The function of sol-gel processing in those methods is to coat templates with thin metal oxide films [160–184].

4. THIN FILM DEPOSITION TECHNIQUES

Uniform, conformal thin films of different materials (metals, oxides, nitrides etc.) are widely applicable in modern technology. In particular, thin films have been used in wide variety of applications, like semiconductor devices [200], wireless communications [201], integrated circuits [202], transistors [203], solar cells [204], light-emitting diodes [205], magneto-optic memories [206], electro-optic coatings [207], multilayer capacitors [208], flat-panel displays [209], nano electromechanical systems (NEMS) [200], micro electromechanical systems (MEMS) [200], multifunctional emerging coatings and gas sensors [201]. These are only few possible applications, the number is growing rapidly. Several techniques have been applied to obtain thin layers of different materials, such as: physical vapor deposition (PVD), pulsed laser deposition (PLD), sol-gel chemistry, chemical vapor deposition (CVD) (Figure 11) [112]. As it appears in this list, the thin film techniques can be divided into several categories: liquid phase and gas phase techniques; physical process and chemical process (Figure 11). The principle of physical deposition techniques is the evaporation or ejection of the precipitated material from the source, whereas chemical deposition methods depend on the physical properties. Unfortunately, all these methods meet significant drawbacks when large areas with rough surface need to be coated with very thin and uniform layers of another material. For example, in CVD, growth mostly leads to particle agglomeration and uniform deposition of large surface areas is often limited by the depletion of precursor. PVD is line-of-sight film deposition technique and do not allow conformal deposition. Sol-gel chemistry, although superb for obtaining very complex structures at very small scale, is not practicable at uniform coating of high aspect ratio structures and surfaces with trenches. Common denominator of these methods is uncontrollable deposition rate. However, last few decades have been a real triumph for the thin film technique called atomic layer deposition (ALD), historically also known as atomic layer epitaxy (ALE) [213]. ALD allows to coat even very complex structures and rough surfaces with extremely uniform films. The main advantage of this deposition technique is a high precision control over the film thickness. ALD is also possible to carry out at lower temperatures, compared with CVD and PLD [214–216]. This allows to use biological substrates as well. And moreover, the ALD is easily transferred to industrial lines. In recent years it has proved itself as a reliable technique for growing of high dielectrics for ultrascaled complementary metal oxide semiconductor (CMOS) devices [217].

| Common thin film deposition methods | | |
|---|---|---|
| Liquid phase | Gas phase | |
| <ul style="list-style-type: none"> • Spin coating • Dip coating • Chemical solution deposition (CSD) • Electroless deposition • Electroplating (ECD) • Liquid-phase epitaxy | Physical vapor deposition (PVD) | Chemical deposition techniques |
| | <ul style="list-style-type: none"> • Vacuum evaporation • Electron-beam evaporation • Sputter deposition • Cathodic arc deposition • Pulsed laser deposition (PLD) | <ul style="list-style-type: none"> • Chemical vapor deposition (CVD) • Vapor phase epitaxy (VPE) • Atomic layer deposition (ALD) • Atomic layer epitaxy (ALE) |
| | <ul style="list-style-type: none"> • Molecular beam epitaxy (MBE) | |

Figure 11. Deposition techniques of thin films.

4.1. Atomic layer deposition

Although the processes similar to the atomic layer deposition were investigated already in the 1960s, the year of birth of ALD is considered to be 1977. In this year Finnish scientists T. Suntola and M.J. Antson granted a first patent – atomic layer epitaxy of compound thin films [218]. However, it was recognized later that W.B. Aleskowskii from Russia reported about ALD-related phenomena, surface processes of TiCl_4 and GeCl_4 on hydrated silica, prior to Suntola [219]. Due to the quick commercialization of results obtained by Suntola, the ALD began to spread to the world from Finland.

Atomic layer deposition is a sequential, self-limiting gas-phase deposition technique. The principle of ALD is alternating saturating surface reactions. During the ALD process, the substrate material is exposed to precursor vapor that forms a (sub)monolayer of the precursor material on the surface of substrate. Subsequently the precursor vapor is removed from the reaction chamber by a purging with inert gas (argon, nitrogen etc.). Then, the reactant gas (H_2O vapor, O_3) is pulsed to the reaction chamber, where it reacts with the adsorbed layer of precursor material and is followed by another purge of inert gas to clean the reaction chamber for first precursor (Figure 12). By introducing precursor materials into reaction chamber in such a manner, no gas-phase reaction occurs. And thus, the film is grown layer-by-layer onto substrate. It is clear that in this case the thickness of the film can be controlled very accurately, merely by the number of deposition cycles. The principle of ALD is illustrated on the figure 13. Purging not only prevents reactions between two precursors, but also removes reaction byproducts of surface reactions from the reactor and therefore limits the formation of impurities in the grown film. However, the term *atomic layer deposition* may be in some cases a certain sense of misconception, because in real deposition processes often the single cycle results less than a monolayer of the desired material due to the steric hindrance of the precursors.

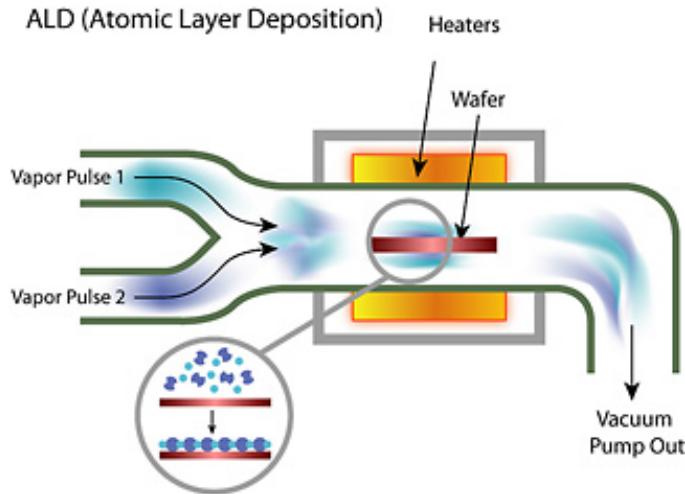


Figure 12. Schematic representation of an ALD reactor [227].

The unique process characteristics and good controllability have made the ALD for the best technique for growing conformal, uniform thin films with precise thickness control and composition over large areas with rough topology [220–224]. Since precursors come together only at the surface of the substrate, very reactive precursors can be applied, which makes ALD chemically very versatile technique.

In the ALD process it is important that the monolayer is formed by the chemisorbing of precursor molecules onto the surface of the substrate. In other words, the precursor molecules have to form chemical bonds with functional groups at the substrate. This distinguishes the ALD from other deposition techniques, like PVD, where the precursor molecules are physisorbed on the substrate surface by much weaker van der Waals forces. The deposition of only one monolayer is ensured by the purge of the reaction chamber with inert gas. During this procedure, all precursor molecules which are not chemisorbed, but physisorbed on the desired monolayer, are removed from the chamber.

In different film deposition techniques, the film growth rate is an important parameter, referring directly to the speed of the process in time-continuous deposition techniques and thus, also to its practicality. In ALD, however, the measure named *growth per cycle* (GPC) is used. It represents the increase of the thickness of deposited film within one complete ALD cycle. The GPC is usually very small, therefore ALD is more suitable for ultra thin film applications with film thicknesses usually less than hundred nm [213–224].

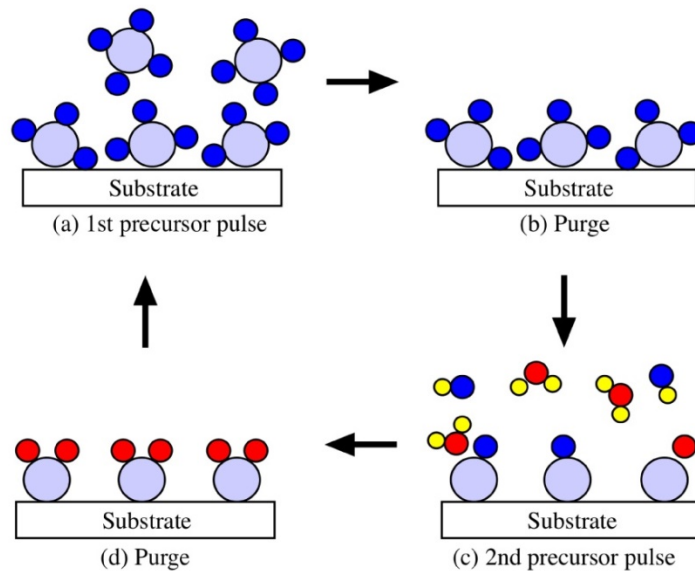


Figure 13. Schematic representation of an ALD process [228].

Because the ALD is a chemical process, the nature of the precursors is of utmost relevance. Precursors used in ALD must meet certain requirements: adequate reactivity to ensure efficient surface reactions; volatility; thermal stability; resistance to decomposition at the film surface [221–224]. Common precursors in ALD are alkoxides and diketonates [224]. One requirement for the surface reactions in ALD process is that the reactions must be complementary. By this is meant that precursors must prepare the surface reactive for the other precursor vapour. Only in this case the cycles can be repeated. Hydroxyl groups on the surface of substrate are the initiating sites for the film growth. It could be assumed that one precursor molecule react with one -OH group. But the relations between the amount of chemisorbed precursor molecules and temperature dependence of -OH densities have been more thoroughly investigated on the example of HfCl_4 and SiO_2 . It was found that if the -OH density is less than 2.2 -OH/nm^2 , each precursor molecule reacts with one -OH site. But above 2.9 -OH/nm^2 , two or even three -OH sites are needed to react with one HfCl_4 molecule [225]. The substrate in the ALD process have influence only on the first few growth cycles, until one monolayer is formed.

5. RESULTS AND DISCUSSION

5.1. Precursor materials

5.1.1 Preparation of metal-oxo-alkoxide sols

The paper I in the list of original papers of current thesis can be considered as an origin or the starting point of the thesis. In this paper, synthesis of sol-gel precursors is discussed. The structure of ready-to-use precursors is studied using SAXS, FTIR, NMR and XRD methods. The preparation of gel fibres from precursors is demonstrated and discussed. The paper focuses on the limitations of direct drawing as fibres preparation method. Paper IV is about formation of hollow fibres (microtubes, capillaries). The differences between the formation mechanisms of gel fibres and hollow gel fibres are experimentally shown and discussed. Paper III focuses on mechanical properties (Young's modulus and tensile strength) of gel fibres. The story focuses on evolution of these parameters during the aging and thermal treatment of fibres. Paper II is a discussion about crack formation during the gellification of sols and post treatments. The topic is important as the cracking is one of the most serious drawbacks of sol-gel technology. Maximum diameter of fibres and microtubes (and bulkiness of sol-gel materials in general) is defined by cracking. Paper V is discussion about properties of microtubes important in applications under external conditions (high temperature, high pressure and plasma applied inside of the tube). The properties of the tubes important for ionic membrane application in solid oxide fuel cells (SOFC) is discussed. A single tube based plasma device is demonstrated. Paper VI focuses on optical properties of Sm^{3+} and Eu^{2+} doped of yttria stabilised zirconia doped microtubes and on their potential applications as light emitting materials. Paper VII is a demonstration of atomic layer deposition of MgO on the surface of microtubes. The coatings are required for the functionalisation of the tubes in order to take them into use in construction of SOFC or micro plasma chambers. Paper VIII (a patent) focuses on explanation of differences between our approach to microtubes preparation and its closest analogues.

5.1.2. Formation, structure and chemistry of metal alkoxides based sol-precursors

It is known earlier that nonhydrolysed metal alkoxides exist as molecular tri- or tetramers. In paper II it is shown that 0–0.7 moles of additional water is needed to transform metal alkoxides into spinnable (spinnability is defined as a property needed to draw the matters into long slender threads), crucial in fibres preparation from metal-oxo alkoxide precursors. The exact quantity depends on nature of alkoxide, mainly on stability of particles that is in a correlation with structure of used alkoxy groups. In the paper II, it is concluded that in the experiments carried out, the following mole quantities of water are to be added

to the metal alkoxide in order to transfer these into spinnable metal-oxo-alkoxide sols:

| Alkoxide | <i>R</i> |
|----------------------|-------------------|
| Sn(OBu) ₄ | 0.5–0.8 |
| Sn(OPr) ₄ | 0.2–0.3 (decomp.) |
| Ti(OBu) ₄ | 0.6–0.9 |
| Ti(OPr) ₄ | 0.5–0.8 |
| Zr(OBu) ₄ | 0.4–0.6 |
| Zr(OPr) ₄ | 0.4–0.6 |
| Hf(OBu) ₄ | 0.4–0.6 |
| Ce(OBu) ₄ | 0 |
| Ce(OPr) ₄ | 0 |

It should be noted also that it is not an easy task to control the rate of metal alkoxide hydrolysis. We can even propose that it can be done by controlling the spinnability of alkoxides as a result of addition of water. For example, we have noticed that alkoxides purchased from different manufacturers may turn or not turn spinnable as a result of adding different quantities of water. In the case of Zr-butoxide, this quantity would vary from 0.2 to 0.7 moles of water per a mole of alkoxide. This is probably related to different rates of hydrolysis of commercial metal alkoxides.

In 1950s, Don Bradley [16] used cryoscopic and ebullioscopic molar mass detection methods to study clusters of metal-oxo-alkoxides, formed as a result of addition of water. Nowadays the structure can be studied by different modern techniques, such as SAXS, SEM, TEM, XRD, FTIR, NMRm, etc. that we have also applied to study our materials. The main results introduced in the different papers are listed in the table below:

| Method used for analysis | Results | Paper |
|--------------------------|---|--------------|
| SAXS | Hydrolysed and thermally treated Sn(OBu) ₄ particles have elongated shapes, with a 3.5–4.5 nm length and 1.2–1.6 nm diameter Water-treated Sn(OBu) ₄ precursors contain ~1nm size particles. The volume distribution function of particles in the hydrolyzed Ti(OBu) ₄ was calculated by assuming a spherical particle shape model. | I III |
| XRD | Analysis did not detect any crystalline phases in water treated Sn(OBu) ₄ fiber precursors. Precursors prepared by thermal treatment of Sn(OBu) ₄ shown broad reflections. | I |
| FTIR | Water and thermal treatment of Sn(OBu) ₄ led to the growth of the 465 cm ⁻¹ peak that is associated with Sn–O vibrations. | I |
| NMR | Shown transition of 6-coordinated Sn into 5-coordinated Sn during the heat-treatment of Sn(OBu) ₄ | I |

It can be concluded that all the methods demonstrated that our precursor materials consist slightly crystalline or amorphous nanoparticles, 2–4 nm in size. The results are in a good correlation with MTSAL theory proposed by professor Vadim Kessler [12], a co autor of our paper IV. In accord with the theory, addition of water to metal alkoxides leads to profound changes in their structure. Alkoxy groups that act as stabilizing shell around metal-oxo cores are released as a result of hydrolysis. Thereafter particles undergo growth to bigger sizes which also stabilise their structure. The hydrolysis and growth of particles is explained by extremely high acidity of metal alkoxides in the Lewis sense, which appears to be the driving force of self-agglomeration. This directs towards the increase of particle size and, therefore, the increase of viscosity. Alkoxide groups in this action play a role as templates, defining the shape, structure and stability of particles. Therefore, the concept is named as Molecular Templated Self-Assembly of Ligands (MTSAL).

5.1.3. Fibres vs. Tubes drawing.

It is shown in Paper I that the drawing of fibres is a typical chemical technology process where the precursor properties are crucial. The main demand for the precursors is spinnability, defined as the ability of liquid to form threads under application of external stress, mechanical or electrostatic (electrospinning) forces. The second requirement is the possibility to transform viscous precursor threads into solid fibres, which is usually achieved via drying (dry pulling), cooling (melt pulling), osmosis (wet pulling) or as a result of chemical reactions. It is shown in Paper I that as-synthesized as well as heat-treated and water-treated $\text{Sn}(\text{OBu})_4$ exhibit a typical behaviour of non-Newtonian liquids: apparent dynamic viscosity decreases with the shearing rate. This is characteristic behaviour for polymeric liquids and can be explained by the alignment and sliding of elongated particles under applied stress. The shear thinning behaviour was more pronounced for the water treated samples, compared to the heat treated ones. Tin butoxide precursors have a higher storage G^0 modulus (elastic response) than loss G^{00} modulus (viscous response) indicating a predominantly elastic behaviour. The frequency dependence of the moduli is polynomial for both the water and heat-treatment-processed systems; the power exponents of G^0 for the water treated and heat-treated samples are 0.14 and 0.03, respectively, and both exponents are 0.15 for G^{00} . A low value of the G^0 exponent indicates higher elasticity, thus the intermolecular cross-links are stronger for the heat-treated than water-treated precursors.

Paper IV focuses on solidification occurring as a result of chemical processes of liquid threads drawn into air. The paper is built up as a discussion about different mechanisms of solidification leading to formation of fibers in the case of $\text{Ti}(\text{OBu})_4$ and hollow fibres in case of $\text{Zr}(\text{OBu})_4$. The metal-oxo-alkoxide liquid threads, when pulled out from the bulb into a humid atmosphere were immediately jacketed by a solid shell that formed on the outer surface via

hydrolysis–condensation of the precursor and coalescence of the resulting nanoparticles. The solidification proceeded during the entire reaction of the precursor. During the solidification, sol–gel material shrinks and loses volume as a result of several processes such as evaporation of solvents, crystallization, and tighter packaging or coalescence of particles. In our experiments the volume loss (shrinkage) of the fibers during the solidification process was measured *in situ*. The higher shrinkage in the case of Zr-alkoxides (~15% of volume) is certainly due to the increase in the coordination number of Zr from 6 to 8 during the process, inducing formation of denser particles compared to Ti-alkoxide that shrinks just 3–4% of volume, and their tighter packing. In the case of Ti derivatives, no coordination number change occurred and it remained equal to 6 during the complete process of solidification.

We have shown that both metal-oxo cores and length of alkoxy groups stabilizing the surface of the cores, induce a dissimilar behaviour in curing: Zr-alkoxide threads formed tubes whereas curing of Ti-alkoxide threads transformed into solid fibers. The solidification process for Ti-oxo-alkoxide threads in humid air is rather trivial. It starts from the surface and proceeds uniformly in time until the whole liquid content is transformed into inhomogeneous solid in the form of a long slender fiber (Fig. 6, Paper IV). Explanation for the curing of Zr-butoxide liquid threads is that these solidify as a result of gelation and form a hollow region to the core as a result of the syneresis process occurring inside the shell. In this case, the tube walls form during the homogeneous densification process of metal-oxo gel in a butanol medium. The driving force of the solidification process is the growth of a number of bonds between the metal-oxo-cores, which forces the released liquid phase butanol to diffuse out from the Zr-oxo solid network that is pronouncedly polar and basic by its nature as explained. As the outer surface of the thread has formed previously as a highly dense and rigid shell, the only option to shrink and reduce the volume during the syneresis process remains to press released butanol into the core along the axis of the fibers. The latter idea is indirectly supported by the fact that higher amounts of organics are preserved within the material produced from Zr-butoxide compared to Ti-butoxide.

In addition, the fact that the tubes formed from Zr-butoxide are structurally homogeneous, while the tubes formed from Zr-propoxide show up as a layered structure, supports the proposed hypothesis that shorter propoxide ligands form thermodynamically less stable layer on the surface of the particles than longer butoxide ligands. This stability is manifested even in the thermal behaviour of the aged microtubes as can be seen from their thermogravimetric analysis. The higher stability of the protective layer induces a slower growth rate allowing the formation of a denser layer. On the other hand, propanol molecules are smaller, which makes it a better solvent with lower viscosity than butanol (2.3 cP and 2.98 cP at 20 °C respectively) and thus also facilitating the growth. The separation of the phases in butanol is therefore limited and the conditions remain homogeneous during the curing of threads. The alternative explanation for the curing of Zr-butoxide liquid threads is that these solidify homogeneously as a

result of gelation and form a hollow region in the core as a result of the syneresis process. In that case, the tube walls form during the densification process of metal-oxo gel in a butanol medium. The driving force of the solidification process is the growth of a number of bonds between the metal-oxo-cores, which forces the released liquid phase butanol to diffuse out from the Zr-oxo solid network that is pronouncedly polar and basic by its nature as explained. As the outer surface of the thread has formed previously as a highly dense and rigid shell, the only option to shrink and reduce the volume during the syneresis process remains to press released butanol into the core along the axis of the fibres. The latter idea gets an indirect confirmation from the fact that higher amounts of organics are preserved within the material produced from zirconium butoxide compared to titanium butoxide.

5.2. Post-processing: monitoring of structure and properties during the aging and heat treatment of fibres and tubes

In order to transform sol-gel-prepared materials into fully dense metal oxide nanoceramics, ageing and heat-treatment procedures were performed (Papers I-VII). The treatments led to the removal of organics from the material and cause additional densification and crystallisation, which improves the mechanical characteristics of materials important in their applications: Young modulus and tensile strength achieved higher values (Paper III).

The mechanical tests performed on as-prepared TiO_2 fibers obtained from corresponding butoxides indicated tensile strength within 3–6 MPa range. These rather low values can be explained by the absence of strong bonding in the 3D network between metal-oxo particles as building blocks of the material. As already discussed above, contrary to the as-prepared ZrO_2 microtubes, the as-prepared TiO_2 fibers can be dissolved in hexane just after solidification without strong bridging bonds and therefore justify the low value. Aging of these structures induces a densification and formation of the bridging bonds between the particles, which in turn leads to an increase of tensile strength up to the range from 200 to 300 MPa. However, aged TiO_2 materials showed tensile strength 2 times higher than that in aged ZrO_2 microtubes, featuring strong interparticle bonding already in as-prepared materials. The tensile strength of aged ZrO_2 microtubes is about 100–150 MPa. Young modulus of both aged TiO_2 and ZrO_2 materials is about 4–5 GPa.

Analyses done in order to study post processing of metal oxide tubes and fibres is listed below:

| Method used for analysis | Results | Paper |
|---|---|--|
| Method | The main result or observation | Published |
| AFM | Demonstrated smoothness of fibres in 1–2 nm scale | Paper I |
| Monitoring and theoretical discussion about cracks formation in aging sol-gel materials | | paper II |
| Measurements of mechanical properties | Young modulus of both aged TiO ₂ and ZrO ₂ materials is about 4–5 GPa. Tensile strength of TiO ₂ fibres is 200 to 300 MPa. Tensile strength of ZrO ₂ tubes is 100–150 MPa ZrO ₂ tubes can withstand 1000 atm overpressure applied inside the microtubes | Paper III Paper III Paper III Paper V |
| Thermo gravimetry | Monitoring of release of organics during the heat-treatment. | Paper IV |
| SEM analysis | The surface of ZrO ₂ microtubes is nanoscale homogeneous | Papers IV,V |
| XRD analysis | Crystallinity of fibres and tubes grows from some nanometers up to some tens of nanometers as a result of thermal treatment up to 1000 °C. Addition of 8% of yttria into zirconia enables to fully stabilize its structure and obtain 100% tetragonal nanocrystalline material. | Papers IV,V Paper V |

The analyses demonstrate evolution of structural properties of materials: the growth of crystallites, their densification and phase structural changes, release of organics and residuals of carbon.

5.2.1. Functional properties and applications of final materials.

Our papers demonstrated that sol-gel process, if carried out properly, enables to prepare metal oxide materials which are structurally homogeneous in nanoscale. Structural homogeneity of final materials were demonstrated and discussed in Papers I, and III-VI. It was shown in Paper I that SnO₂ fibres can be prepared homogeneously in nanoscale and therefore optically transparent, usefully, e.g., for possible applications as waveguides. The structural uniformity ensures acceptable waveguiding properties of the fibres, and the optical losses measured in the ZrO₂ fibres with diameter of 3 μm were smaller than 1 dBmm⁻¹.

It was demonstrated that the incorporation of rare earth metal ions into synthesised sol-gel materials allows one to enhance their luminescent properties in the visible range. It was shown in Papers V and VI that the temperature dependence of the average lifetime of Eu^{3+} fluorescence decay detected at the 606 nm peak of the $5\text{D}_0 \rightarrow 7\text{F}_2$ emission possess fluorescence based temperature detection.

Paper III was focused on evolution of mechanical properties of ZrO_2 microtubes and TiO_2 fibres during the post-synthesis heat treatment. Tests were carried out on individual fibers to measure their elastic modulus and the tensile strength as functions of processing conditions. The modulus of elasticity of as-fabricated fibers increased about 10 times after calcination at $700\text{ }^\circ\text{C}$, while the strain at failure remained almost the same at $\sim 1.4\%$. The highest tensile strength of 833 MPa was exhibited by nanoscale grained fiber with a bimodal grain size distribution consisting of rutile grains embedded in anatase matrix. This two-phase nanocrystalline structure may have reduced the critical defect size, and thus increased the tensile strength. These values support the potential application of the materials under extreme conditions. It was demonstrated in paper V that the tube walls can withstand at least up to 1000 atm oil pressure inside the tubes. The tubes can also be easily manipulated and bent slightly with micro manipulators. When the tube is melt-jointed to the top of glass pipette in the flame then it can be used later to touch different surfaces hard enough to visually observe its bending under applied force. These properties possess application for example in microfluidic systems under extreme conditions. It was demonstrated in paper V that high mechanical and thermal stability of microtubes enable their use in individual tubes based plasma devices.

Impedance spectroscopic methods enabled to demonstrate that the ionic conductivity of yttria stabilized zirconia microtubes is 0.05 S cm^{-1} at $1000\text{ }^\circ\text{C}$, which is somewhat lower than $0.09\text{--}0.13\text{ S cm}^{-1}$, i.e. lower than the widely accepted typical range of the experimentally determined YSZ conductivity values. However, in the literature much lower conductivities are also presented, depending on the microstructure (density of the grain boundaries) of the YSZ phase studied. It was shown also that there is no short-circuiting between measuring electrodes in the set-up, allowing one to rely on the insignificant electronic conductivity in this material. The fact that synthesised YSZ microtubes meet both criteria - they are ionically conductive with no electronic component and also mechanically stable at higher temperatures in addition, the tubes can be proposed for ionic membrane application in solid oxide fuel cell engineering. The tubes have a potential to miniaturize microtubular solid oxide fuel cell concept for 500 times in terms of cross-sectional area of the elements. Miniaturization of these elements in this scale would possibly possess several orders of magnitude shorter start-up times and several orders of magnitude higher power output values per volume of SOFC systems.

6. SUMMARY AND CONCLUSIONS

High aspect ratio, up to 10 000, fine metal oxide fibres can directly be drawn from concentrated metal alkoxide precursors. Fibres with diameter as small as 200 nm could be achieved. That low value is earlier proposed as ultimate limit for direct drawing from polymeric solutions. Rheological tests proved that proposed metal alkoxide precursors behave as non-Newtonian fluids. The observed shear thinning flow behaviour could be explained by sliding of supra-molecular linear shape aggregates of the material under applied external stress.

Almost solventless liquid nanoparticulate Zr-oxo-alkoxide precursor, when trapped inside the rigid shell (formed as a result of crosslinking of precursor particles on the surface of drawn jet), undergoes reactions leading to a loss of the stabilising alkoxy layer from the surface of the nanoparticles. The alkoxy groups are released when the particles get in contact with the water that diffuses to the reaction zone through the shell. In the large enough quantity of released alcohol, the released particles can self-assemble and make the shell thicker by saturating on its inner surface. Finally, ageing and thermal annealing treatments induce the transition of as-prepared microtubular materials into dense nanoceramics. After thermal treatment oxide microtubes possess excellent mechanical properties: the tubes, up to 100 microns in thickness, up to 20 micron in wall thickness and length up to several cm, achieve high tensile strength (600–800 MPa) and Young modulus (up to 150 GPa).

We have shown that yttrium stabilized zirconium oxide microtubes with metastable tetragonal crystalline phase can be functionalized in atomic layer deposition processes. MgO thin film deposition from β -diketonate-type precursor $\text{Mg}(\text{thd})_2$ was carried out on YSZ microtubes which makes them applicable in miniature plasma-jet-devices. MgO films were grown to thickness of approximately 15 nm on the tube surface with the growth rate of 0.1 Å/cycle.

It is proposed that the observed mechanisms open a broad horizon regarding the preparation of novel materials and application of potentially useful devices made of them. Among the most evident candidates for the creation of tubular structures is HfO_2 which is a compound is very similar to ZrO_2 . Moreover, we have already made some preliminary tests and shown that the same can be expected in the case of oxides of rare earth metals. Our tests have shown that the tubes have suitable properties for high temperature ionic membrane applications like solid oxide fuel cells (SOFC) or gas sensors. Advantage of proposed microtubes in those applications is related to the increment of the active surface area, small thickness of electrolyte, higher mechanical stability and enhanced power output per volume unit. We have also demonstrated that the tubes are promising in construction of miniature plasma jet systems. Advantages of the tubes in this application are related to their proper dimensions and high mechanical stability. In addition, we have shown that the tubes are promising candidates as media for light generation constituting, for example, light emitting diodes (LED).

7. SUMMARY IN ESTONIAN

Kombineeritud sool-geel ja aatomkihtsadestatud struktuurid

Kõrge, kuni kümne tuhandeni ulatava aspektisuhtega ehk kõrge pikkuse ja dia-meetri suhtega metalloksiidfiibreid võis vahetult nukleerida ja venitada välja metallalkoksiidlähteainete kontsentratsioonist. Sel meetodil sünteesiti isegi kuni 200-nanomeetrilise läbimõõduga fiibreid. Nii väikest läbimõõtu on juba varem peetud fiibrile polümeersetest lahustest väljavenitamisel saavutatavaks absoluutseks piiriks. Reoloogilised testid tõestasid seejuures, et metallalkoksiidlähteained käituvad nn. mitte-Newtoni vedelikena. Tuvastatud nihke-vedeldusefektist mõjutatud materjalikogumi kitsenemist selle voolamisel võiks seletada supermolekulaarsete lineaarsete ahelate tekke ja kogunemisega ning omavahe-lise libisemisega välise mehhaanilise pinge rakendumisel (klaaspulgaga prekursormaterjalist fiibreid tõmmates).

Jäigastunud kooriku sisse lõksustunud peaaegu lahustivaba nanoosakeseline tsirkooniumi oksoalkoksiidlähteaine allutatakse reaktsioonidele, mis viivad osakesi stabiliseeriva alkoksü-rühmade kihi kadumiseni nanoosakeste pinnalt. Koorik siinjuures oli moodustunud lähteaine osakeste aglomereerumisel piki lähteainest väljavenitatava joa ja kaas moodustuva fiibrilge pinda. Alkoksü-rühmade vabastamine pinnalt toimub osakeste kokkupuutel veega, mis difundeerub reaktsioonitsooni läbi kooriku. Kui reaktsioonil vabanenud alkoholi määr on piisavalt kõrge, siis võivad vabanenud osakesed ise rühmituda ja paksendada koorikut küllastades selle sisepinda. Lõpuks, terminine töötlemine ning vanandamine algatavad mikrotorujate materjalikogumite ülemineku tihendatud nanokeraamiliseks materjaliks. Selliseid materjale iseloomustavad juba algselt atraktiivsed mehhaanilised omadused. Kuni 100 mikronini ulatuvate koguläbimõõdude ja 20 mikronini ulatuvate seina läbimõõdudega ning mitmete sentimeetriteni ulatuvate pikkustega torude venitustugevus jääb vahemikku 600–800 MPa ning Young'i moodul ulatub väärtuseni 150 GPa.

Me oleme näidanud, et ütriumiga stabiliseeritud tsirkooniumoksiidist mikro-torusid, mis on kristalliseerunud tetragonaalses tsirkooniumoksiidi faasis, võib edasi funktsionaliseerida aatomkihtsadestusprotsessis. Mikrotorusid võis kon-formselt katta õhukese, ligikaudu 15 nm paksuse magneesiumioksiidikihiga kasutades magneesiumi beeta-diketonaati metallilähteainena. MgO kihiga katmine võimaldaks mikrotorusid tugevdada võimaldamaks neid edaspidi pikema-ajaliselt kasutada miniatuursetes plasmadüüsid. Võib arvata, et töös vaadeldud materjali formeerumise mehhanismid avavad uusi ja laialdasi võimalusi uute materjalide valmistamisel ja nende võimalikul kasulikul rakendamisel. Üks ilm-semaid kandidaate selleks oleks HfO_2 , mis on tsirkooniumoksiidiga väga sar-naste keemiliste ja füüsikaliste omadustega ühend. Veel enam, me oleme teinud ka esimesi katseid, mis näitasid, et samasugust fiibertehnoloogiat võiks raken-dada haruldaste muldmetallide oksiidide puhul. Meie testid on näidanud, et sellistel torudel on omadusi, mis võimaldaksid nende rakendamist tahkisoksiid-põhistes kütuseelementides. Mikrotorude kimpude kasutamise eeldatavad

eelised siinjuures toetuvad sellega kaasnevale aktiivse pindala suurenemisele, õhukese elektrolüüdikihi kasutamise võimalusele, kõrgemale mehhaanisele stabiilsusele ja võimalikult kõrgele elemendi erivõimsusele. Me oleme ka näidanud, et sellised torud on paljulubavad konstruktsioonelemendid miniatuurseid plasmajugasid genereerivates ja juhtivates süsteemides juba nende väikeste dimensioonide ning kõrge mehhaanilise stabiilsuse tõttu. Lisaks oleme näidanud, et sellised torud võivad olla kasulikud valgust genereerivas keskkonnas ja selleks sobilike seadmete nagu valgusdiodide konstrueerimisel.

8. ACKNOWLEDGEMENTS

Foremost, I would like to thank my supervisors Dr. Kaupo Kukli and Dr. Tanel Tättle for their help and support during my Ph.D. studies. Their contribution to the completion of current thesis and papers has been invaluable.

I greatly appreciate all my colleagues and friends from the Institute of Physics and from the Institute of Chemistry. I am very thankful for the valuable scientific discussions with Dr. Aile Tamm. I would like to thank Dr. Hugo Mändar, Dr. Kathriin Utt, Kelly Hanschmidt and Dr. Rasmus Talviste for the characterization of the optical and mechanical properties of the microtubes. Special thanks to Dr. Ants Lõhmus for providing technical advice for the design of experiment devices. Also I want express my thanks to the group of Imaginaarkuivikud for the inspiration and comprehensive support. It was very pleasant to learn and work together with them during these years.

Finally, I would like to thank my family and relatives. I am indescribably grateful that they have supported me in my studies at the university. I am also very grateful to Kristel who have believed in me and supported me.

This work was supported by the following agencies and foundations: Graduate School „Functional materials and technologies“ (European Social Fund project 1.2.0401.090079); ETF9292 „Combined sol-gel and solid-liquid phase separation processes in elaboration of novel shaped metal oxide nanoceramics.“; ETF8377 „Elaboration of tubular microstructures by controlled plastic-elastic transformation of alkoxide surfaces“; SF0180058s07 „Low-dimensional structures and their applications“; SF0180042s07 „Layered structures of solid films for information technology and nanoelectronics“; ETF7612 „Micro and nanosize metal oxide fibres“; TK141 „Advanced materials and high-technology devices for sustainable energetics, sensorics and nanoelectronics“; IUT2-24 „Thin-film structures for nanoelectronic applications and functional coatings“

9. REFERENCES

1. C.B. Carter, M.G. Norton, Ceramic Materials. Science and Engineering. Springer, 2013.
2. V. Santos, M. Zeni, C.P. Bergmann, J.M. Hohemberger. Correlation between thermal treatment and tetragonal/monoclinic nanostructured zirconia powder obtained by sol-gel process. *Review on Advanced Materials Science*, 17 (2008), 62–70.
3. C. Airoidi, R.F. de Farias. Alkoxide as precursors in the synthesis of new materials through the sol-gel process. *Quimica Nova*. 27 (2004), 84–88.
4. C.M. Malengreux, A. Timmermans, S.L. Pirard, S.D. Lambert, J.-P. Pirard, D. Poelman, B. Heinrichs. Optimized deposition of TiO₂ thin films produced by a non-aqueous sol-gel method and quantification of their photocatalytic activity. *Chemical Engineering Journal*, 195–196 (2012), 347–358.
5. C. Lind, S.D. Gates, N.M. Pedoussaut, T.I. Baiz. Novel Materials through Non-Hydrolytic Sol-Gel Processing: Negative Thermal Expansion Oxides and Beyond. *Materials*, 3(4) (2010), 2567–2587.
6. M. Mirzaee, M.M. Amini, M. Sadeghi, F.Y. Mousavi, M. Sharbatdaran. Preparation and characterization of boehmite, CuO, TiO₂ and Nb₂O₅ by hydrothermal assisted sol-gel processing of metal alkoxides. *Ceramics Silikaty*, 49(1) (2005), 40–47.
7. M. Wu, G. Lin, D. Chen, G. Wang, D. He, S. Feng, R. Xu. Sol-Hydrothermal Synthesis and Hydrothermally Structural Evolution of Nanocrystal Titanium Dioxide. *Chemistry of Materials*, 14(5) (2002), 1974–1980.
8. Y. Li, X. Duan, H. Liao, Y. Qian. Self-Regulation Synthesis of Nanocrystalline ZnGa₂O₄ by Hydrothermal Reaction. *Chemistry of Materials*, 10(1) (1998), 17–18.
9. K. Yanagisawa, J.C. Rendon-Angeles, H. Kanai, Y. Yamashita. Stability and single crystal growth of lead scandium niobate and its solid-solution with lead titanate under hydrothermal conditions. *Journal of Materials Science*, 35(12) (2000), 3011–3015.
10. M. Niederberger, N. Pinna. Metal Oxide Nanoparticles in Organic Solvents. Synthesis, Formation, Assembly and Application. Springer, 2009.
11. S. Sakka, Handbook of Sol-Gel Science and Technology; volume I: Sol-Gel Processing. Kluwer Academic Publishers, 2005.
12. O. Ben-David, E. Shafir, I. Gilath, Y. Prior, D. Avnir. Long Term Renewable Sol-Gel Fluorescent Optical Fiber pH Sensor. *SPIE Conference Proceedings*, 3136 (1997), 104 -113.
13. J. Blum and D. Avnir. Catalysis and Reactivity with Sol-Gel Entrapped Organic and Organometallic Chemicals, chapter 33 in Handbook of Sol-Gel Science and Technology, S. Sakka, Kluwer Academic Publishers, 2004.
14. M.C. Caracoche, P.C. Rivas, M.M. Cervera, R. Caruso, E. Benavi'dez, O. de Sanctis, M.E. Escobar. Zirconium Oxide Structure Prepared by the Sol-Gel Route: I, The Role of the Alcoholic Solvent. *Journal of the American Ceramic Society*, 83(2) (2000), 377–384.
15. C.J. Brinker, G.W. Scherer. Sol-gel science, the physics and chemistry of sol-gel processing. Academic Press, San Diego, 1990.
16. M. Kakihana. Sol-Gel preparation of high temperature superconducting oxides. *Journal of Sol-Gel Science and Technology*, 6 (1996), 7–55.

17. M. Rozman, M. Drogenik. Hydrothermal Synthesis of Manganese Zinc Ferrites. *Journal of the American Ceramic Society*, 78 (9) (1995), 2449–2455.
18. Ebelmen: Untersuchungen über die Verbindungen der Borsäure und Kieselsäure mit Aether. *Pharmaceutical Chemistry Journal*, 57 (1846), 334.
19. W. Geffcken, E. Berger. Changing the reflective capacity of optical glass, DE Patent 736411, (1943).
20. H. Dislich, P. Hinz, R. Kaufmann. Preparation of transparent, vitreous, crystalline inorganic multiple component materials, especially in thin layers, at temperatures far below their melting points”, DE Patent 1941191, (1971).
21. H. Dislich. New routes to multicomponent oxide glasses. *Angewandte Chemie International Edition*, 10 (1971), 363–370.
22. H. Dislich. Glassy and Crystalline Systems from Gels: Chemical Basis and Technical Application. *Journal of Non-Crystal Solids*, 57 (1983), 371–388.
23. H. Dislich. Sol gel 1984 → 2004. *Journal of Non-Crystal Solids*, 73 (1985), 599–612.
24. R.J.P. Corriu, D. Leclercq. Recent developments of molecular chemistry for sol-gel processes. *Angewandte Chemie International Edition*, 35 (1996), 1420–1436.
25. J.N. Hay, H.M. Raval. Synthesis of organic-inorganic hybrids via the non-hydrolytic sol-gel process. *Chemistry of Materials*, 13 (2001), 3396–3403.
26. L.L. Hench, J.K. West. The sol-gel process. *Chemical Review*, 90 (1990), 33–72.
27. A. Vioux. Nonhydrolytic sol-gel routes to oxides. *Chemistry of Materials*, 9 (1997), 2292–2299.
28. J.C.-S. Wu, L.-C. Cheng. An improved synthesis of ultrafiltration zirconia membranes via the sol-gel route using alkoxide precursor. *Journal of Membrane Science*, 167 (2000) 253–261.
29. C.J. Brinker, R. Sehgal, S.L. Hietala, R. Deshpande, D.M. Smith, D. Loy, C.S. Ashley, Sol-gel strategies for controlled porosity inorganic materials, *Journal of Membrane Science*, 94 (1994) 85.
30. C. Wolf, C. Rüssel. Sol-gel formation of zirconia: preparation, structure and rheology of sols. *Journal of Materials Science*, 27 (1992), 3749.
31. J. Etienne, A. Larbot, A. Julbe, L. Cot. A microporous zirconia membrane prepared by the sol-gel process from zirconyl oxalate. *Journal of Membrane Science*, 86 (1994), 95.
32. S. Doeuff, M. Henry, C. Sanchez. Sol-gel synthesis and characterization of titanium oxo-acetate polymers *Materials Research Bulletin*, 25(12) (1990), 1519.
33. J. Livage, M. Henry, C. Sanchez. Sol-gel chemistry of transition metal oxides. *Progress in Solid State Chemistry*, 18 (1988), 259–341.
34. M. Niederberger. Nonaqueous sol-gel routes to metal oxide nanoparticles. *Accounts of Chemical Research*, 40 (2007), 793–800.
35. M. Niederberger, M. Antonietti. Nanomaterials chemistry: Recent developments and new directions, chap. Nonaqueous sol-gel routes to nanocrystalline metal oxides, Wiley-VCH, 119–138. (2007).
36. N. Pinna, M. Niederberger. Surfactant-free nonaqueous synthesis of metal oxide nanostructures. *Angewandte Chemie International Edition*, 47 (2008), 5292–5304.
37. E. Matijevic. Monodispersed metal (hydrous) oxides - a fascinating field of colloid science. *Accounts of Chemical Research*, 14(1) (1981), 22–29.
38. S. Zhang, Y. Han, B. Chen, X. Song. *Materials Letters*, 51 (2001), 308.

39. C.D. Chandler, C. Roger, M.J. Hampden-Smith. Chemical aspects of solution routes to perovskite-phase mixed-metal oxides from metal-organic precursors. *Chemical Reviews*, 93 (1993), 1205–1241.
40. V.G. Kessler. The chemistry behind the sol–gel synthesis of complex oxide nanoparticles for bio-imaging applications. *Journal of Sol-Gel Science and Technology*, 51 (2009), 264–271.
41. G.I. Spijksma, G.A. Seisenbaeva, A. Fischer, H.J.M. Bouwmeester, D.H.A. Blank, V.G. Kessler. The molecular composition of non-modified and acac-modified propoxide and butoxide precursors of zirconium and hafnium dioxides. *Journal of Sol-Gel Science and Technology*, 51 (2009), 10–22.
42. C.J. Brinker, G.W. Scherer. *Sol-Gel Science. The Physics and Chemistry of Sol-Gel Processing*. Academic Press, Inc., Boston, San Diego, NY, 1990, 908 pp.
43. A. Pierre. *Introduction in Sol-Gel Processing*. Kluwer, Boston, 1998, 394 pp.
44. J.D. Wright, N.A.J.M. Sommerdijk. *Sol-Gel Materials: Chemistry and Applications*. Taylor and Francis, London, 2001, 125 pp.
45. A.C. Piere, G.M. Pajonk. Chemistry of aerogels and their applications. *Chemical Reviews*, 2002, 102, 4243–4265.
46. J. Livage, M. Henry, C. Sanchez. Sol-gel chemistry of transition metal oxides. *Progress in Solid State Chemistry*, 18 (1988), 259–341.
47. J.P. Jolivet, M. Henry, J. Livage. *Metal Oxide Chemistry and Synthesis – From Solution to Solid State*. J. Wiley & Sons, Ltd. Chichester, New York, Weinheim, 2000, 321 pp.
48. A. Vioux. Nonhydrolytic Sol–Gel Routes to Oxides. *Chemistry of Materials*, 9 (1997), 2292–2299.
49. H.D. Gesser, P.C. Goswami. Aerogels and related porous materials. *Chemical Reviews*, 89 (1989), 765–788.
50. L.L. Hench, J.K. West. The sol-gel process. *Chemical Reviews*, 90 (1990), 33–72.
51. A.C. Pierre. Porous sol-gel ceramics. *Ceramics International*, 23 (1997), 229–238.
52. J. Fricke, T. Tillotson. Aerogels: Production, Characterization and Applications. *Thin Solid Films*, 297 (1997), 212.
53. L.L. Murrel. Sols and mixtures of sols as precursors of unique oxides. *Catalysis Today*, 35 (1997), 225–245.
54. J.B. Miller, E.I. Ko. Control of mixed-oxide textural and acidic properties by the sol-gel method. *Catalysis Today*, 35 (1997), 269–292.
55. N. Hüsing, U. Schubert. Aerogels – Airy Materials: Chemistry, Structure, and Properties. *Angewandte Chemie International Edition*, 37 (1998), 22–45.
56. J. Livage. Sol-gel synthesis of heterogeneous catalysts from aqueous solutions. *Catalysis Today*, 41 (1998), 3–19.
57. T.F. Baumann, A.E. Gash, G.A. Fox, J.H. Satcher, L.W. Hrubesh, in *Handbook of Porous Solids*, F. Schüth, K.S.W. Sing, J. Weitkamp (Eds.), Wiley-VCH, Weinheim, 3 (2002), p. 2014.
58. C. Moreno-Castilla, F.J. Maldonado-Hodar. Carbon aerogels for catalysis applications: An overview. *Carbon*, 43 (2005), 455–465.
59. A.W. Dearing, E.E. Reid. Alkyl orthosilicates. *Journal of American Chemical Society*, 50 (1928), 3058–3062.
60. H. Dislich, P. Hinz, R. Kaufmann. U.S. Patent 3,759,683; Sept. 18, 1973; assigned to Jenaer Glaswerk Schott and Gen.
61. M.J. Harnpden-Smith, T.A. Wark, C.J. Brinker. The solid state and solution structures of tin(IV) alkoxide compounds and their use as precursors to form tin

- oxide ceramics via sol-gel-type hydrolysis and condensation. *Coordination Chemistry Reviews*, 112 (1992) 81–116.
62. Schroeder, H. and Gliemeroth, G., U.S. Patent 3,597,252; August 3, 1971; assigned to Jenaer Glaserk Schott and Gen.
 63. T. Schneller, R. Waser, M. Kosec, D. Payne. *Chemical Solution Deposition of Functional Oxide Thin Films*. Springer 2013.
 64. P.J. Flory. *Principles of Polymer Chemistry*, Cornell University Press, 1953.
 65. P.J. Flory. *Faraday Discussions of the Chemical Society*. 57 (1974), 7–18.
 66. E.M. Rabinovich. *Sol-Gel Technology for Thin Films, Fibers, Preforms, Electronics and Speciality Shapes*, ed. E.C. Klein, Noyes 1988, 260–294.
 67. C. J. Brinker, G. W. Scherer. *Sol-Gel Science – The Physics and Chemistry of Sol-Gel Processing*, Academic Press, Boston, 1990.
 68. A.C. Pierre. *Introduction to Sol-Gel Processing*, Kluwer Academic Publishers, Boston, 1998.
 69. C.J. Brinker, D.E. Clark, D.R. Ulrich, *Better Ceramics Through Chemistry*, North-Holland, New York, 1984.
 70. F.D. Osterholtz, E.R. Pohl. Kinetics of the hydrolysis and condensation of organofunctional alkoxysilanes: a review. *Journal of Adhesion Science and Technology*, 6 (1992), 127–149.
 71. C.J. Brinker. Hydrolysis and Condensation of silicates: Effects on Structure. *Journal of Non-Crystalline Solids* 100 (1988), 31–50.
 72. S.-L. Chen, P. Dong, G.-H. Yang, J.-J. Yang. Kinetics of Formation of Monodisperse Colloidal Silica Particles through the Hydrolysis and Condensation of Tetraethylorthosilicate. *Industrial and Engineering Chemistry Research*, 35 (12) (1996), 4487–4493.
 73. J.K. Bailey, M.L. Mecartney. Formation of colloidal silica particles from alkoxides. *Colloids and Surfaces* 63 (1992), 151–161.;
 74. G.H. Bogush, I.V. Zukoski. Studies of the kinetics of the precipitation of uniform silica particles through the hydrolysis and condensation of silicon alkoxides. *Journal of Colloid Interface Science*, 142 (1991), 1–18.
 75. M.T. Harris, R.R. Brunson. The base-catalyzed hydrolysis and condensation reaction of dilute and concentration TEOS solutions. *Journal of Non-Crystal Solids*, 121 (1990), 397–403.
 76. I.L. Radtchenko, M. Giersig. Inorganic particle synthesis in confined micron-sized polyelectrolyte capsules. *Langmuir*, 18, (21) (2002), 8204–8208.
 77. Y.A. Attia. *Sol-Gel Processing and Applications*. Springer Science 1994.
 78. J.D. Wright, N.A.J.M. Sommerdijk. *Sol-Gel Materials: Chemistry and Applications*. CRC Press 2001.
 79. S. Prabakar, R.A. Assink. Cross-Condensation Kinetics of Organically Modified Silica Sols. *Materials Research Society*, 435 (1996), 345.
 80. M.E. Simonsen, E.G. Sogaard. Sol-gel reactions of titanium alkoxides and water: influence of pH and alkoxy group on cluster formation and properties of the resulting products. *Journal of Sol-Gel Science and Technology*, 53 (2010), 485–497.
 81. J.F. Harrod, R.M. Laine. *Inorganic and Organometallic oligomers and polymers*. Springer Science 1991.
 82. M. Abdelmouleh, M.N. Belgacem, S. Boufi, M.-C. Brochier-Salon, P.A. Bayle. Kinetics of hydrolysis and self-condensation reaction of silanes by NMR

- spectroscopy. *Colloids and Surfaces A: Physicochemical and Engineering Aspects*, Elsevier, 312 (2008), 83–91.
83. J.-K. Park, J.-J. Myoung, J.-B. Kyong, H.-K. Kim. Reaction Mechanism for the Hydrolysis of Titanium Alkoxides. *Bulletin of Korean Chemical Society*, 24 (5) (2003), 671–673.
 84. N.Y. Turova, E.P. Turevskaya, V.G. Kessler, M.I. Yanovskaya. *The Chemistry of Metal Alkoxides*. Kluwer Academic Publishers 2002.
 85. A.E. Danks, S.R. Hall, Z. Schnepf. The evolution of ‘sol–gel’ chemistry as a technique for materials synthesis. *Materials Horizon*, 3 (2016), 91–112.
 86. R. Trbojevič, N. Pellegrini, A. Frattini, O. de Sanctis. Preparation and isolation of gold nanoparticles coated with a stabilizer and sol-gel compatible agent. *Journal of Materials Research*, 17 (8) (2002), 1973–1980.
 87. K. Majid, R. Mushtaq, S.Ahmad. Synthesis, Characterization and Coordinating Behaviour of Aminoalcohol Complexes with Transition Metals. *E-Journal of Chemistry*, 5 (2008), 969–979.
 88. E.Y. Tsui, J.S. Kanady, M.W. Daya, T. Agapie. Trinuclear first row transition metal complexes of a hexapyridyl, trialkoxy 1,3,5-triarylbenzene ligand. *Chemical Communications*, 47 (2011), 4189–4191.
 89. D.C. Bradley, R.C. Mehrotra, J.D. Swanwick, W. Wardlaw. Structural chemistry of the alkoxides. Part IV. Normal alkoxides of silicon, titanium, and zirconium. *Journal of Chemical Society*, 1953, 2025–2030.
 90. S. Takenaka, R. Takahashi, S. Sato, T. Sodesawa. Structural Study of Mesoporous Titania Prepared from Titanium Alkoxide and Carboxylic Acids. *Journal of Sol-Gel Science and Technology*, 19 (2000), 711.
 91. D. Raoufi, T. Raoufi. The effect of heat treatment on the physical properties of sol–gel derived ZnO thin films. *Applied Surface Science*, 255 (2009), 5812–5817.
 92. S.H. Hakim, B.H. Shanks. A Comparative Study of Macroporous Metal Oxides Synthesized via a Unified Approach. *Chemistry of Materials*, 21 (2009), 2027–2038.
 93. D.R. Ulrich. Prospects of sol-gel processes. *Journal of Non-Crystal Solids*, 100 (1988), 174–193.
 94. G.R. Lee, J.A. Crayston. Sol-gel processing of transition-metal alkoxides for electronics. *Advanced Materials*, 5 (6) (1993), 434–442.
 95. S.K. Young. Sol-Gel Science for Ceramic Materials. *Material Matters*, 8 (2006).
 96. K.K. Banger, Y. Yamashita, K. Mori, R.L. Peterson, T. Leedham, J. Rickard, H. Siringhaus. Low-temperature, high-performance solution-processed metal oxide thin-film transistors formed by a ‘sol–gel on chip’ process. *Nature Materials*, 10 (2011), 45–50.
 97. M. Järvekülg, R. Vålbe, J. Jõgi, A. Salundi, T. Kangur, V. Reedo, J. Kalda, U. Mäeorg, A. Lõhmus, A.E. Romanov. A sol-gel approach to self formation of microtubular structures from metal oxide gel films. *Physica Status Solidi A*, 209, 12 (2012), 2481–2486.
 98. T. Tätte, V. Reedo, T. Avarmaa, R. Lõhmus, U. Mäeorg, M.E. Pistol, J. Subbi, A. Lõhmus. Metal oxide based SPM tips prepared by sol-gel method. *Physics of Low-Dimensional Structures*, 5–6 (2002), 31–37.
 99. T. Tätte, M. Paalo, V. Kisand, V. Reedo, A. Kartushinsky, K. Saal, U. Mäeorg, A. Lõhmus, I. Kink. Pinching of alkoxide jets – a route for preparing nanometre level sharp oxide fibres. *Nanotechnology*, 18 (2) (2007), 125–301.

100. L.G. Hubert-Pfalzgraf. Some aspects of homo and heterometallic alkoxides based on functional alcohols. *Coordination Chemistry Reviews*, 178–180 (1998), 967–997.
101. J.N. Hay, H.M. Raval. Synthesis of organic-inorganic hybrids via the nonhydrolytic sol-gel process. *Chemistry of Materials*, 13 (2001), 3396–3403.
102. M. Inoue, H. Kominami, T. Inui. Novel synthetic method for the catalytic use of thermally stable zirconia: Thermal decomposition of zirconium alkoxides in organic media. *Applied Catalysis, A* 97 (1993), 25–30.
103. M. Inoue, H. Kominami, H. Otsu, T. Inui. Synthesis of microcrystalline titania in organic media. *Nippon Kagaku Kaishi* (1991), 1364–1366.
104. M. Jansen, E. Guenther. Oxide gels and ceramics prepared by a nonhydrolytic sol-gel process. *Chemistry of Materials*, 7 (1995), 2110–2114.
105. J.P. Jolivet. Metal oxide chemistry and synthesis – from solution to solid state. *John Wiley & Sons Ltd.*, Chichester, England (2000).
106. R.C. Mehrotra, A. Singh. Recent trends in metal alkoxide chemistry. *Progress in Inorganic Chemistry*, 46 (1997), 239–454.
107. M. Niederberger. Nonaqueous sol-gel routes to metal oxide nanoparticles. *Accounts of Chemical Research*, 40 (2007), 793–800.
108. M. Niederberger, M. Antonietti. Nanomaterials chemistry: Recent developments and new directions, chap. Nonaqueous sol-gel routes to nanocrystalline metal oxides, *Wiley-VCH*, (2007) 119–138.
109. T.J. Trentler, T.E. Denler, J.F. Bertone, A. Agrawal, V.L. Colvin. Synthesis of TiO₂ nanocrystals by nonhydrolytic solution-based reactions. *Journal of American Chemical Society*, 121 (1999), 1613–1614.
110. N.Y. Turova, E.P. Turevskaya. The chemistry of metal alkoxides. *Kluwer Academic Publishers*, Boston (2002).
111. J.A. Ibers. Refinement of a linear group: direct refinement of an interatomic bond length. *Acta Crystallographica*, 27 (1971), 250–251.
112. J.A. Ibers. Crystal and Molecular Structure of Titanium (IV) Ethoxide. *Nature*, 197 (1963), 686 – 687.
113. D.C. Bradley, D.G. Carter, Metal Oxide Alkoxide Polymers: Part III. The Hydrolysis of Secondary and Tertiary Alkoxides of Zirconium. *Canadian Journal of Chemistry*, 40 (1962), 15–21.
114. D.C. Bradley, E.V. Caldwell, W.J. Wardlaw, *Chemical Society*, 79 (1957), 4775.
115. D.C. Bradley, R.C. Mehrotra, I.P. Rothwell, A. Singh, *Alkoxo and Aryloxo Derivatives of Metals*, Elsevier, New York, 2001.
116. J. Livage, M. Henry, C. Sanchez. Sol-gel chemistry of transition metal oxides. *Progress in Solid State Chemistry*, 18 (1988), 259–342.
117. H. Fric, U. Schubert. *Journal of Sol–Gel Science and Technology*, 48:2 (2008).
118. R. Lichtenberger, U. Schubert, Chemical modification of aluminium alkoxides for sol-gel processing. *Journal of Materials Chemistry*, 20 (2010), 9287–9296.
119. U. Schubert, N. Hüsing, *Synthesis of inorganic materials*, Wiley-VCH, Weinheim, 2000.
120. V.W. Day, T.A. Eberspacher, Y. Chen, J. Hao, W.G. Klemperer. Low-nuclearity titanium oxoalkoxides: the trititanates [Ti₃O](OPri)₁₀ and [Ti₃O](OPri)₉(OMe). *Inorganica Chimica Acta*, 229 (1995), 391–405.
121. W.J. Evans, M.A. Ansari, J.W. Ziller. Isolation and structural characterization of the polymetallic zirconium alkoxide complexes, Zr₃O(OCH₂CMe₃)₉Cl, Zr₃O(OCMe₃)₉(OH), and Na₄Zr₆O₂(OEt)₂₄. *Polyhedron*, 17 (1998), 869–877.

122. A. Mosset, I. Gautier-Luneau, J. Galy. Sol-gel processed BaTiO₃: Structural evolution from the gel to the crystalline powder. *Journal of Non-Crystalline Solids*, 100 (1988), 339–344.
123. V.W. Day, T.A. Eberspacher, W.G. Klemperer, C.W. Park, F.S. Rosenberg. Solution structure elucidation of early transition metal polyoxoalkoxides using oxygen-17 NMR spectroscopy. *Journal of the American Chemical Society*, 113 (21) (1991), 8190–8192.
124. D.C. Bradley. In: Stone FGA and Graham WAG (eds) Inorganic polymers. Academic Press, New York, (1962), 444.
125. A. Mueller, E. Krickemeyer, H. Boegge, M. Schmidtman, F. Peters, C. Menke, J. Meyer. An unusual polyoxomolybdate: giant wheels linked to chains. *Angewandte Chemie International Edition English*, 36 (1997):484.
126. A. Mueller, E. Krickemeyer, H. Boegge, M. Schmidtman, M. Beugholt, S.K. Das, F. Peters. Giant ring-shaped building blocks linked to form a layered cluster network with nanosized channels: [Mo₁₂₄^{VI}Mo₂₈^VO₄₂₉(μ₃-O)₂₈H₁₄(H₂O)_{66.5}]¹⁶⁻. *Chemistry: A European Journal*, 5 (1999):1496.
127. A. Mueller, S.Q.N. Shah, H. Boegge, M. Schmidtman. Molecular growth from a Mo₁₇₆ to Mo₂₄₈ cluster. *Nature*, 397 (1999):48.
128. A. Mueller, S.K. Das, V.P. Fedin, E. Krickemeyer, C. Beugholt, H. Boegge, M. Schmidtman, B. Hauptfleisch. Rapid and simple isolation of the crystalline molybdenum-blue compounds with discrete and linked nanosized ring-shaped anions: Na₁₅[Mo^{VI}₁₂₆Mo^V₂₈O₄₆₂H₁₄(H₂O)₇₀]_{0.5}[Mo^{VI}₁₂₆Mo^V₂₈O₄₅₇H₁₄(H₂O)₆₈]_{0.5} ca. 400 H₂O and Na₂₂[Mo^{VI}₁₁₈Mo^V₂₈O₄₄₂H₁₄(H₂O)₅₈] ca. 250 H₂O. *Zeitschrift für Anorganische und Allgemeine Chemie*, 625:1187 (1999).
129. A. Muller, A.M. Todea, H. Bogge, J. van Slageren, M. Dressel, A. Stammler, M. Rusu. Formation of a „less stable“ polyanion directed and protected by the electrophilic internal surface functionalities of a capsule in growth: [(Mo₆O₁₉)²⁻ → (Mo^{VI}₇₂Fe^{III}₃₀O₂₅₂(ac)₂₀(H₂O)₉₂]⁴⁻. *Chemical Communications*, 29 (2006), 3066.
130. M.J. Lundqvist, M. Nilsing, P. Persson, S. Lunell, DFT study of bare and dye-sensitized TiO₂ clusters and nanocrystals. *International Journal of Quantum Chemistry*, 106 (2006), 3214–3234.
131. P. Persson, J.C.M. Gebhardt, S. Lunell, The Smallest Possible Nanocrystals of Semiionic Oxides. *Journal of Physical Chemistry B*, 107 (2003), 3336–3339.
132. S. Kozhukharov. Relationship between the conditions of preparation by the sol-gel route and the properties of the obtained products. *Journal of the University of Chemical Technology and Metallurgy*, 44, 2, (2009), 143–150.
133. M.D.C. Serrano, S. Kozhukharov. Application of the sol-gel techniques for obtaining of new multifunctional materials, Development – Future Perspectives and Innovations in the Science, Proc., Sofia, 2006, 84–93.
134. Y.M. Rodionov, E.M. Slyusarenko, V.V. Lunin, *Russian Chemistry Reviews*, 65 (1996), 797.
135. G. Arrachart, D.J. Cassidy, I. Karatchevtseva, G. Triani, Nanostructural Evolution of Titania-Based Materials Using Modified Titanium Precursors, *Journal of American Ceramic Society*, 92 (2009) 2109–2115.
136. H. Choi, E. Stathatos, D.D. Dionysiou, Synthesis of nanocrystalline photocatalytic TiO₂ thin films and particles using sol-gel method modified with nonionic surfactants, *Thin Solid Films*, 510 (2006) 107–114.

137. F. Babonneau, L. Coury, J. Livage. Aluminum sec-butoxide modified with ethylacetoacetate: an attractive precursor for the sol-gel synthesis of ceramics. *Journal of Non-Crystal Solids*, 121 (1990), 153–157.
138. S. Rezgui, B.C. Gates. Sol-Gel Synthesis of Alumina in the Presence of Acetic Acid: Distinguishing Gels and Gelatinous Precipitates by NMR Spectroscopy. *Chemistry of Materials*, 6 (1994), 2386.
139. F. Vaudy, S. Khodabandeh, M.E. Davis. Synthesis of pure alumina mesoporous materials. *Chemistry of Materials*, 8 (1996), 1451–1464.
140. A. Alipour, H. Jazayeri, A. Nemati, M.M. Amini. Preparation of submicron alumina from aluminum 2-methoxyethoxide. *Materials Letters*, 48 (2001), 15–20.
141. M.K. Hubbert. Darcy's Law and the field equations of the flow of underground fluids. *International Association of Scientific Hydrology. Bulletin*, 2, 23–59.
142. J. Zarzycki, M. Prassas, J. Phalippou. Synthesis of glasses from gels: the problems of monolithic gels. *Journal of Materials Science*, 17 (1982), 3371–3379.
143. E. Rivera-Muñoz, W. Brostow, R. Rodríguez, V.M. Castaño. Growth of hydroxyapatite on silica gels in the presence of organic additives: kinetics and mechanism. *Materials Research Innovations*, 4 (2001), 222–230.
144. S.S. Kistler. Coherent Expanded Aerogels and Jellies. *Nature*, 127 (1931), 741.
145. S.S. Kistler. Coherent expanded aerogels. *Journal of Physical Chemistry*, 36 (1932), 52–64.
146. G.A. Nicolaon, S.J. Teichner. Preparation of silica aerogels from methyl orthosilicate in alcoholic medium, and their properties. *Bulletin de la Societe Chimique de France*, (1968) 1906–1911.
147. Z. Zhao, X. Jiaoa, D. Chen. Preparation of TiO₂ aerogels by a sol-gel combined solvothermal route. *Journal of Materials Chemistry*, 19 (2009), 3078–3083.
148. M.A. Aegerter et al., *Aerogels Handbook, Advances in Sol-Gel Derived Materials and Technologies*. Springer Science 2011.
149. T. Heinrich, U. Klett, J. Fricke. Aerogels—Nanoporous materials part I: Sol-gel process and drying of gels. *Journal of Porous Materials*, 1 (1995), 7–17.
150. R. Sui, A.S. Rizkalla, P.A. Charpentier. Synthesis and Formation of Silica Aerogel Particles By a Novel Sol–Gel Route in Supercritical Carbon Dioxide. *Journal of Physical Chemistry B*, 108 (2004), 11886–11892.
151. A.E. Gash, T.M. Tillotson, J.H. Satcher, L.W. Hrubesh, R.L. Simpson. New Sol-Gel Synthetic Route to Transition and Main-Group Metal Oxide Aerogels using Inorganic Salt Precursors. Sixth International Symposium on Aerogels, Albuquerque, NM, October 8–11, 2000.
152. S.C. Warren, M.R. Perkins, A.M. Adams, M. Kamperman, A.A. Burns, H. Arora, E. Herz, T. Suteewong, H. Sai, Z. Li, J. Werner, J. Song, U. Werner-Zwanziger, J.W. Zwanziger, M. Grätzel, F.J. DiSalva, U. Wiesner. A silica sol–gel design strategy for nanostructured metallic materials. *Nature Materials*, 11 (2012), 460–467.
153. A.V. Rao, S.D. Bhagat, H. Hirashima, G.M. Pajonk. Synthesis of flexible silica aerogels using methyltrimethoxysilane (MTMS) precursor. *Journal of Colloid and Interface Science*, 300 (2006), 279–285.
154. H. Kozuka. Fundamental issues on solgel coatings – stress evolution, cracking and radiative striation. In: H. Kozuka, ed. *Kluwer Academic Publishers 2004*, 247–307. *Handbook of sol-gel science and technology vol.1.*

155. P. Innocenzi, H. Kozuka, S. Sakka. Preparation of coating films doped with gold metal particles from methyltriethoxysilane-tetraethoxysilane solutions. *Journal of Sol-Gel Science and Technology*, 1 (1994), 305–318.
156. G. Zhao, H. Kozuka, S. Sakka. Preparation of TiO₂ coating films containing Pd fine particles by sol-gel method. *Journal of Sol-Gel Science and Technology*, 4 (1995), 37–47.
157. M. Kawashita, S. Tsuneyama, F. Miyaji, T. Kokubo, H. Kozuka, K. Yamamoto. Antibacterial silver-containing silica glass prepared by sol-gel method. *Bio-materials*, 21 (2000), 393–398.
158. H. Kozukaa, M. Takahashib, K. Niinuraa, H. Uchiyama. Fabrication of highly crystalline oxide thin films on plastics: Sol-gel transfer technique involving high temperature process. *Journal of Asian Ceramic Societies*, 4 (2016), 329–336.
159. T.J. Garino. The Cracking of Sol-Gel Films During Drying. *MRS Proceedings*, 180 (1990), 497.
160. P. Hoyer. Formation of a Titanium Dioxide Nanotube Array. *Langmuir*, 12 (6) (1996), 1411–1413.
161. V.M. Cepak, J.C. Hulteen, G. Che, K.B. Jirage, B.B. Lakshmi, E.R. Fischer, C.R. Martin. Chemical Strategies for Template Syntheses of Composite Micro and Nanostructures. *Chemistry of Materials*, 9 (5) (1997), 1065–1067.
162. M. Terrones, N. Grobert, J. Olivares, J.P. Zhang, H. Terrones, K. Kordatos, W.K. Hsu, J.P. Hare, P.D. Townsend, K. Prassides, A. K. Cheetham, H.W. Kroto, D.R.M. Walton. Controlled production of aligned-nanotube bundles. *Nature*, 388 (1997), 52–55.
163. Q. Peng, X.-Y. Sun, J.C. Spagnola, G.K. Hyde, R.J. Spontak, G.N. Parsons. Atomic Layer Deposition on Electrospun Polymer Fibers as a Direct Route to Al₂O₃ Microtubes with Precise Wall Thickness Control. *Nano Letters*, 7 (2007), 719–722.
164. R.A. Caruso, J.H. Schattka, A. Greiner. Titanium Dioxide Tubes from Sol-Gel Coating of Electrospun Polymer Fiber. *Advanced Materials*, 13 (2001), 1577–1579.
165. M. Bognitzki, H.Q. Hou, M. Ishaque, T. Frese, M. Hellwig, C. Schwarte, A. Schaper, J.H. Wendorff, A. Greiner. Polymer, metal, and hybrid nano- and mesotubes by coating of degradable polymer templates (TUFT-process). *Advanced Materials*, 12 (2000), 637–640.
166. D.A. Czaplewski, J. Kameoka, R. Mathers, G.W. Coates, H.G. Craighead. Nanofluidic channels with elliptical cross sections formed using a nonlithographic process. *Applied Physics Letters*, 83 (2003), 4836–4838.
167. J. Kameoka, S.S. Verbridge, H. Liu, D.A. Czaplewski, H.G. Craighead. Fabrication of suspended silica glass nanofibers from polymeric materials using a scanned electrospinning source. *Nano Letters*, 4 (2004), 2105–2108.
168. H. Dong, S. Prasad, V. Nyame, W.E. Jones. Sub-micrometer conducting polyaniline tubes prepared from polymer fiber templates. *Chemistry of Materials*, 16 (2004), 371–373.
169. Z. Pajkic, M. Willert-Porada. Synthesis and Characterization of Alumina Microtubes in a Template Process from Short Carbon Fibers. *Advanced Engineering Materials*, 9 (2007), 381–384.
170. J.W. Kim, S.W. Myoung, H.C. Kim, J.H. Lee, Y.G. Jung, C.Y. Jo. *Materials Science and Engineering*, A434 (2006), 171.
171. P. Gibot, C. Vix-Guterl. TiO₂ and [TiO₂/β-SiC] microtubes prepared from an original process. *Journal of European Ceramic Society*, 27 (2007), 2195–2201.

172. D. Yang, L. Qi, J. Ma. Hierarchically ordered networks comprising crystalline ZrO₂ tubes through sol-gel mineralization of eggshell membranes. *Journal of Materials Chemistry*, 13 (2003), 1119–1123.
173. J. Bao, C. Tie, Z. Xu, Q. Zhou, D. Shen, Q. Ma. Template Synthesis of an Array of Nickel Nanotubes and Its Magnetic Behavior. *Advanced Materials*, 13 (2001), 1631–1633.
174. M. Daub, M. Knez, U. Goesele, K. Nielsch. Ferromagnetic nanotubes by atomic layer deposition in anodic alumina membranes. *Journal of Applied Physics*, 101 (2007), 09, 111.
175. J. Bachmann, J. Jing, M. Knez, S. Barth, H. Shen, S. Mathur, U. Goesele, K. Nielsch. Ordered iron oxide nanotube arrays of controlled geometry and tunable magnetism by atomic layer deposition. *Journal of American Chemical Society*, 129 (2007), 9554–9555.
176. P. Gao, P. Zhan, M. Liu. Controlled synthesis of double-and multiwall silver nanotubes with template organogel from a bolaamphiphile. *Langmuir*, 22 (2006), 775–779.
177. T. Peng, H. Yang, K. Dai, K. Nakanishi, K. Hirao. Sol-Gel Template Synthesis of Aluminum Oxide Microtubes. *Advanced Engineering Materials*, 6 (2004), 241–244.
178. Y. Ono, K. Nakashima, M. Sano, Y. Kanekyio, K. Inoue, J. Hojo, S. Shinkai. Organic Gels are Useful as a Template for the Preparation of Hollow-Fiber Silica. *Chemical Communications*, (1998), 1477–1478.
179. C.N.R. Rao, B.C. Satishkumar, A. Govindaraj. Zirconia nanotubes. *Chemical Communications*, (1997) 1581–1582.
180. J. Bao, D. Xu, Q. Zhou, Z. Xu, Y. Feng, Y. Zhou. An array of concentric composite nanostructure of metal nanowires encapsulated in zirconia nanotubes: preparation, characterization, and magnetic properties. *Chemistry of Materials*, 14 (2002), 4709.
181. C.J. Brumlik and C.R. Martin. Template synthesis of metal microtubules. *Journal of American Chemical Society*, 113 (1991), 3174–3175.
182. T. Kijima, T. Yoshimura, M. Uota, T. Ikeda, D. Fujikawa, S. Mouri, S. Uoyama. Noble-Metal Nanotubes (Pt, Pd, Ag) from Lyotropic Mixed-Surfactant Liquid-Crystal Templates. *Angewandte Chemie International Edition*, 43 (2004), 228–232.
183. M. Lovett, C. Cannizzaro, L. Daheronc, B. Messmera, G. Vunjak-Novakovice, D.L. Kaplana. *Biomaterials*, 28 (2007), 5271.
184. C. Giordano, M.T. Todaro, M. Palumbo, L. Blasi, L. Errico, A. Salhi, A. Quattieri, G. Gigli, A. Passaseo, M. De Vittorio. Hybrid polymer/semiconductor microtubes: a new fabrication approach. *Microelectronics Engineering*, 85 (2008), 1170–1172.
185. P. Colombo, K. Perini, E. Bernardo, T. Capelletti, G. Maccagnan. Ceramic Microtubes from Pre ceramic Polymers. *Journal of American Ceramic Society*, 86 (2003), 1025–1027.
186. W.P. Hoffman, H.T. Phan, P.G. Wapner. The Far-Reaching Nature of Microtube Technology. *Materials Research Innovations*, 2 (1998), 87–96.
187. S. Motojima, W. In-Wang, X. Chen. Preparation and Properties of Microcoils and Microtubes of NbC/C/NbC~NbC by Vapor Phase Metallizing of the Regular Carbon Microcoils. *Materials Research Bulletin*, 35 (2000), 1517–1524.

188. Y. Sun, G.M. Fuge, N.A. Fox, D.J. Riley, M.N.R. Ashfold. Synthesis of aligned arrays of ultrathin ZnO nanotubes on a Si wafer coated with a thin ZnO film. *Advanced Materials*, 17 (2005), 2477–2481.
189. H. Cheng, J. Cheng, Y. Zhang, Q.J. Wang. *Journal of Crystal Growth*, 299 (2007), 34.
190. S. Poehnitzsch, G. Gratwohl. The Development of the Central Pore Canal during Sintering of Ceramic Capillaries. *Practische Metallographie*, 37 (2000), 608–618.
191. X. Yang, L. Wang, S. Yang. *Materials Letters*, 61 (2007), 2904–2907.
192. C.Kayaa, S. Blackburn. Extrusion of ceramic tubes with complex structures of non-uniform curvatures made from nano-powders. *Journal of the European Ceramic Society*, 24 (2004), 3663–3670.
193. C. Kaya, S. Blackburn, Facile route to fabricate large-scale silver microtubes. *Journal of the European Ceramic Society*, 24 (2004), 3663.
194. X. Huang, S. Blackburn, *Key Engineering Materials*, 206 (2001), 433.
195. M. Järvekülg, R. Vålbe, J. Jõgi, A. Salundi, T. Kangur, V. Reedo, J. Kalda, U. Mäeorg, A. Lõhmus, A.E. Romanov. A sol-gel approach to self-formation of microtubular structures from metal alkoxide gel films. *Physica Status Solidi A*, 209, 12 (2012), 2481–2486.
196. E.B. Urena, Y. Mei, E. Coric, D. Makarov, M. Albrecht, O.G. Schmidt. Fabrication of ferromagnetic rolled-up microtubes for magnetic sensors on fluids. *Journal of Physics D: Applied Physics*, 42 (2009).
197. K. Kumar. Polymer, Metal, and Ceramic Microtubes by Strain-driven Self-rolling. Dissertation, Technischen Universität Dresden.
198. M. Akiyama, K. Shobu, C.-N. Xu, K. Nonaka, T. Watanabe. Ceramic microtubes self-formed at room temperature that exhibit a large bending stress. *Journal of Applied Physics*, 88 (2000)
199. X. Zhang, X.N. Jiang, C. Sun. Micro-stereolithography of polymeric and ceramic microstructures. *Sensors and Actuators*, 77 (1999), 149–156.
200. A.I. Kingon, J.P. Maria, S.K. Streiffer. Alternative dielectrics to silicon dioxide for memory and logic devices. *Nature*, 406 (2000), 1032–1038.
201. R.E. Zeng Acosta, L.T. Romankiw, L.J. VonGutfeld. *Thin Solid Films*, 95 (1982),131.
202. M.A. Alam, R.K. Smith, B.E. Weir, P.J. Silverman. Thin dielectric films: Uncorrelated breakdown of integrated circuits. *Nature*, 420 (2002), 378.
203. S. Bolat, Z. Sisman, A.K. Okyay. Demonstration of flexible thin film transistors with GaN channels. *Applied Physics Letters*, 109 (2016).
204. I.M. Dharmadasa. *Advances in Thin-Film Solar Cells*. Pan Stanford Publishing, 2012.
205. Z. Shaohua, F. Bo, Sun Qian, Z. Hanmin. Preparation of GaN-on-Si based thin-film flip-chip LEDs. *Journal of Semiconductors*, 34 (2013).
206. Y. Togami, K. Kabayashi, M. Kajiuura, K. Sato, T. Teranishi. Amorphous Thin Film Disk For Magneto-Optical Memory. Proceedings in SPIE 0329, Optical Disk Technology, 208 (1982).
207. G. Yi, Z. Wu, M. Sayer. Preparation of Pb(Zr,Ti)O₃ thin films by sol gel processing: Electrical, optical, and electro-optic properties. *Journal of Applied Physics*, 64 (2016), 2717.
208. G.L. Brennecka, C.M. Parish, B.A. Tuttle, L.N. Brewer. Multilayer thin and ultrathin film capacitors fabricated by chemical solution deposition. *Journal of Materials Research*, 23 (2008), 176–181.

209. U. Betz, M.K. Olsson, J. Marthy, M.F. Escolá, F. Atamny. Thin films engineering of indium tin oxide: Large area flat panel displays application. *Surface and Coatings Technology*, 200 (2006), 5751–5759.
210. A.V. Sumant, O. Auciello, R.W. Carpick, S. Srinivasan, J.E. Butler. Ultrananocrystalline and Nanocrystalline Diamond Thin Films for MEMS/NEMS Applications. *MRS Bulletin*, 35 (2010).
211. G. Korotchenkov, V. Brynzari, S. Dmitriev. SnO₂ films for thin film gas sensor design. *Materials Science and Engineering: B*, 63 (1999), 195–204.
212. F.U. Hamelmann. Thin film zinc oxide deposited by CVD and PVD. *Journal of Physics: Conference Series*, 764.
213. M. Ritala, M. Leskelä. Atomic layer epitaxy - a valuable tool for nanotechnology? *Nanotechnology*, 10 (1999).
214. J. Aarik, A. Aidla, A.A. Kiisler, T. Uustare, V. Sammelselg. Influence of substrate temperature on atomic layer growth and properties of HfO₂ thin films. *Thin Solid Films*, 340 (1999), 110–116.
215. J. Aarik, A. Aidla, H. Mändar, T. Uustare, V. Sammelselg. Growth kinetics and structure formation of ZrO₂ thin films in chloride-based atomic layer deposition process. *Thin Solid Films*, 408 (2002), 97–103.
216. K. Kukli, M. Ritala, M. Leskelä, J. Sundqvist, L. Oberbeck, J. Heitmann, U. Schröder, J. Aarik, A. Aidla. Influence of TiO₂ incorporation in HfO₂ and Al₂O₃ based capacitor dielectrics. *Thin Solid Films*, 515 (2007), 6447–6451.
217. M. Putkonen, L. Niinistö. Zirconia thin films by atomic layer epitaxy. A comparative study on the use of novel precursors with ozone. *Journal of materials Chemistry*, 11 (2001), 3141–3147.
218. T. Suntola and M. J. Antson, Method for producing compound thin films, Patent, US 4,058,430, 1977.
219. A. Shevjakov, G. Kusnetsowa, and W. Aleskovskii, Interactions of the tetrachlorides of titanium and germanium with hydrated silicon oxide”, in Chemistry of High-Temperature Materials. Proceedings, 2nd USSR Conference on High-Temperature Chemistry of Oxides (26–29 Nov. 1965). 149–155, Nauka, Leningrad, 1967.
220. J. Niinistö, M. Putkonen, L. Niinistö, K. Arstila, T. Sajavaara, J. Lu, K. Kukli, M. Ritala, M. Leskelä. HfO₂ films grown by ALD using cyclopentadienyl-type precursors and H₂O or O₃ as oxygen source. *Journal of the Electrochemical Society*, 153 (2006), F39-F45.
221. J. Niinistö, M. Putkonen, L. Niinistö, F. Song, P. Williams, P.N. Heys, R. Odedra. Atomic layer deposition of HfO₂ thin films exploiting novel cyclopentadienyl precursors at high temperatures. *Journal of Materials Chemistry*, 19 (2007), 3319–3324.
222. J. Niinistö, K. Kukli, M. Kariniemi, M. Ritala, M. Leskelä, N. Blasco, A. Pinchart, C. Lachaud, N. Laaroussi, Z. Wang, C. Dussarrat. Novel mixed alkylamido-cyclopentadienyl precursors for ALD of ZrO₂ thin films. *Journal of Materials Chemistry*, 18 (2008), 5243–5247.
223. K. Kukli, M. Ritala, T. Sajavaara, J. Keinonen, M. Leskelä. Atomic layer deposition of hafnium dioxide films from hafnium tetrakis (ethylmethanamide) and water. *Chemical Vapor Deposition*, 8 (2002), 199–204.
224. K. Kukli, T. Pilvi, M. Ritala, T. Sajavaara, J. Lu, M. Leskelä. Atomic layer deposition of hafnium dioxide thin films from hafnium tetrakis(dimethanamide) and water. *Thin Solid Films*, 491 (2005), 328–338.

225. T. Blanquart. Atomic Layer Deposition of Groups 4 and 5 Transition Metal Oxide Thin Films: Focus on Heteroleptic Precursors. Dissertation, University of Helsinki, 2013.
226. H. Alles, J. Aarik, A. Aidla, A. Fay, J. Kozlova, A. Niilisk, M. Pärs, M. Rähn, M. Wiesner, P. Hakonen, V. Sammelseig. Atomic layer deposition of HfO₂ on graphene from HfCl₄ and H₂O. *Open Physics*, 9 (2011), 319–324.
227. J. Joel. Atomic Layer Deposition Market Growth, Trends, Absolute Opportunity and Value Chain 2014–2020 by SMR. Vacuum Deposition Coatings. Updated on Jun 27, 2016.
228. A.R. Barron. [http://cnx.org/contents/rimBK1xx@2/Atomic-Layer Deposition](http://cnx.org/contents/rimBK1xx@2/Atomic-Layer+Deposition), 23.12.2016.

10. PUBLICATIONS

CURRICULUM VITAE

Name: Marko Part
Date of birth: March 8, 1986
Nationality: Estonian
E-mail: marko.part.86@gmail.com

Education:
2009–2011 University of Tartu MSc (materials science)
2005–2009 University of Tartu BSc (materials science)
1993–2005 Loksa 1. Secondary School

Career:
2016– Estonian Accreditation Centre
2014–2015 University of Tartu, Institute of Physics, engineer
2008–2009 Estonian Nanotechnology Competence Center, laboratory assistant

List of publications:

1. T. Tätte, M. Hussainov, M. Paalo, **M. Part**, R. Talviste, V. Kiisk, H. Mändar, K. Põhako, T. Pehk, K. Reivelt, M. Natali, J. Gorauskis, A. Lõhmus, U. Mäeorg, Alkoxide-based precursors for direct drawing of metal oxide micro- and nanofibres, *Sci. Technol. Adv. Mater.*, 12 (2011) 034412.
2. T. Tätte, A. L. Kolesnikova, M. Hussainov, R. Talviste, R. Lõhmus, A. E. Romanov, I. Hussainova, **M. Part**, A. Lõhmus, Crack formation during post-treatment of nano- and microfibres by sol-gel technique, *J. Nanosci. Nanotechnol.*, 10 (2010) 6009–6016.
3. K. Hanschmidt, T. Tätte, I. Hussainova, **M. Part**, H. Mändar, K. Roosalu, I. Chasiotis, Optimization of mechanical strength of titania fibers fabricated by direct drawing, *Appl. Phys. A*, 113 (2013) 663–671.
4. **M. Part**, K. Hanschmidt, J. Jõgi, E. Rauwel, G. A. Seisenbaeva, V. G. Kessler, T. Tätte, Study of the curing mechanism of metal alkoxide liquid threads for the synthesis of metal oxide fibers or microtubes, *RSC Adv.*, 4 (2014) 12545–12554.
5. T. Tätte, **M. Part**, R. Talviste, K. Hanschmidt, K. Utt, U. Mäeorg, I. Jõgi, V. Kiisk, H. Mändar, G. Nurk, P. Rauwel, Yttria stabilized zirconia microtubes for microfluidics under extreme conditions, *RSC Adv.*, 4 (2014) 17413–17419.
6. K. Utt, **M. Part**, T. Tätte, V. Kiisk, M. G. Brik, A. A. Chaykin, I. Sildos, Spectroscopic properties of Eu-doped Y-stabilized ZrO₂ microtubes, *J. Lumin.*, 152 (2014) 125–128.
7. **M. Part**, A. Tamm, J. Kozlova, H. Mändar, T. Tätte, K. Kukli, Atomic layer deposition of MgO films on yttria-stabilized zirconia microtubes, *Thin Solid Films*, 553 (2014) 30–32.
8. Invention: A Method of Preparing Metal Oxide Microtubes; Tanel Tätte, **Marko Part**, Uno Mäeorg, Valter Kiisk, Gunnar Nurk, Aleksei Vorobjov, Kelli Hanschmidt. Priority number: P201000097; Priority date: 31.12.2010.

ELULOOKIRJELDUS

Nimi: Marko Part
Sünniaeg: 8. märts, 1986
Kodakondsus: Eesti
E-post: marko.part.86@gmail.com

Haridus:
2009–2011 Tartu Ülikool, Tehnikateaduste magister (materjaliteadus)
2005–2009 Tartu Ülikool, Tehnikateaduste bakalaureus (materjaliteadus)
1993–2005 Loksa 1. Keskkool

Töökogemus:
2016- Eesti Akrediteerimiskeskus
2014–2015 Tartu Ülikooli Füüsika Instituut, insener
2008–2009 Eesti Nanotehnoloogiarenduskeskuse AS, laborant

Publikatsioonide loetelu:

1. T. Tätte, M. Hussainov, M. Paalo, **M. Part**, R. Talviste, V. Kiisk, H. Mändar, K. Põhako, T. Pehk, K. Reivelt, M. Natali, J. Gurauskis, A. Lõhmus, U. Mäeorg, Alkoxide-based precursors for direct drawing of metal oxide micro- and nanofibres, *Sci. Technol. Adv. Mater.*, 12 (2011) 034412.
2. T. Tätte, A. L. Kolesnikova, M. Hussainov, R. Talviste, R. Lõhmus, A. E. Romanov, I. Hussainova, **M. Part**, A. Lõhmus, Crack formation during post-treatment of nano- and microfibres by sol-gel technique, *J. Nanosci. Nanotechnol.*, 10 (2010) 6009–6016.
3. K. Hanschmidt, T. Tätte, I. Hussainova, **M. Part**, H. Mändar, K. Roosalu, I. Chasiotis, Optimization of mechanical strength of titania fibers fabricated by direct drawing, *Appl. Phys. A*, 113 (2013) 663–671.
4. **M. Part**, K. Hanschmidt, J. Jõgi, E. Rauwel, G. A. Seisenbaeva, V. G. Kessler, T. Tätte, Study of the curing mechanism of metal alkoxide liquid threads for the synthesis of metal oxide fibers or microtubes, *RSC Adv.*, 4 (2014) 12545–12554.
5. T. Tätte, **M. Part**, R. Talviste, K. Hanschmidt, K. Utt, U. Mäeorg, I. Jõgi, V. Kiisk, H. Mändar, G. Nurk, P. Rauwel, Ytria stabilized zirconia microtubes for microfluidics under extreme conditions, *RSC Adv.*, 4 (2014) 17413–17419.
6. K. Utt, **M. Part**, T. Tätte, V. Kiisk, M. G. Brik, A. A. Chaykin, I. Sildos, Spectroscopic properties of Eu-doped Y-stabilized ZrO₂ microtubes, *J. Lumin.*, 152 (2014) 125–128.
7. **M. Part**, A. Tamm, J. Kozlova, H. Mändar, T. Tätte, K. Kukli, Atomic layer deposition of MgO films on yttria-stabilized zirconia microtubes, *Thin Solid Films*, 553 (2014) 30–32.
8. Invention: A Method of Preparing Metal Oxide Microtubes; Tanel Tätte, **Marko Part**, Uno Mäeorg, Valter Kiisk, Gunnar Nurk, Aleksei Vorobjov, Kelli Hanschmidt. Priority number: P201000097; Priority date: 31.12.2010.

DISSERTATIONES SCIENTIAE MATERIALIS UNIVERSITATIS TARTUENSIS

1. **Martin Järvekülg.** Tubular microstructures by Hf-, Zr- and Ti-butoxide gel sheet rolling. Tartu, 2011, 112 p.
2. **Sergei Vlassov.** Investigation of nanoscale interactions and mechanical properties of nanostructures using quartz tuning fork based real-time measurements. Tartu, 2011, 171 p.
3. **Margus Kodu.** Pulsed Laser Deposition of Magnesium Oxide and Barium Ternary Oxides for Plasma Display Protective Layers. Tartu, 2011, 89 p.
4. **Rainer Pärna.** Surface studies of some oxide films. Tartu, 2011, 129 p.
5. **Jevgeni Šulga.** Self-assembly and interaction of nanostructures. Tartu, 2011, 114 p.
6. **Wojciech Kuznik.** Quantum-chemical computer simulations of the linear and non-linear optical properties of pyrazoloquinoline and dicyanopyrazine derivatives. Tartu, 2012, 89 p.
7. **Leonid Dorogin.** Structural and tribological properties of zero- and one-dimensional nanocrystals. Tartu, 2012, 193 p.
8. **Viljar Palmre.** Fabrication and characterization of microporous carbon-based electroactive polymer actuators. Tartu, 2012, 99 p.
9. **Madis Paalo.** Synthesis of CNT-metal oxide nanocomposites: sol-gel process, rheology, structural and functional properties. Tartu, 2014, 175 p.
10. **Raul Välbe.** Development of ionic liquid composites by sol-gel method for elaboration of industrial nano- and microstructures. Tartu, 2014, 97 p.
11. **Urmas Joost.** Impurity and preparation dependent properties of titania thin films. Tartu, 2014, 155 p.
12. **Madis Umalas.** Application of sol-gel technology for production of ceramic nanocomposites and functional coatings. Tartu, 2015, 136 p.
13. **Elena Samsonova.** Energy transfer probe as a tool to study morphological and structural origins of fluorescence quenching in rare-earth doped nanophosphors. Tartu, 2015, 114 p.
14. **Jay Mondal.** Novel Corrosion Protective Nanostructured Composite Coatings. Tartu, 2016, 104 p.
15. **Kathriin Utt.** Metal oxide mesostructures for optical applications. Tartu, 2016, 88 p.
16. **Kaido Siimon.** Electrospun gelatin cross-linked by glucose. Tartu, 2016, 84 p.